JOC Article

Modulation of Pyrene Fluorescence in DNA Probes Depends upon the Nature of the Conformationally Restricted Nucleotide

Dmytro Honcharenko, Chuanzheng Zhou, and Jyoti Chattopadhyaya*

Department of Bioorganic Chemistry, Box 581, Biomedical Center, Uppsala University, SE-75123 Uppsala, Sweden

jyoti@boc.uu.se

Received December 25, 2007

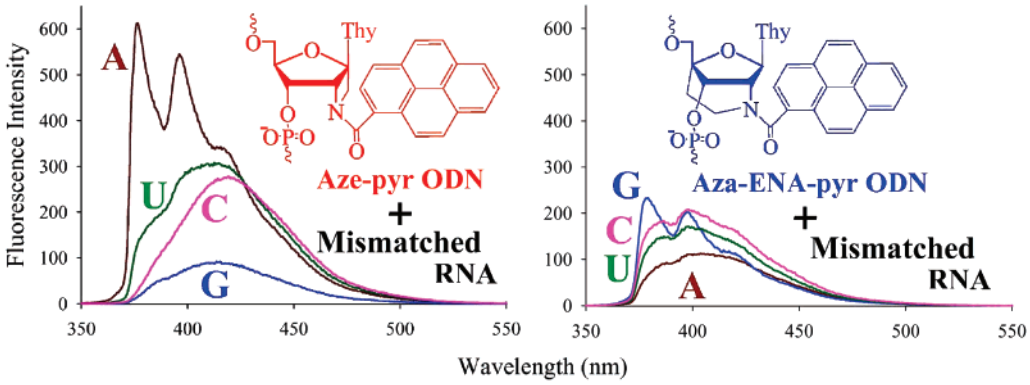

The DNA probes (ODNs) containing a 2′-*N*-(pyren-1-yl)-group on the conformationally locked nucleosides [2′-*N*-(pyren-1-yl)carbonyl-azetidine thymidine, Aze-pyr (**X**), and 2′-*N*-(pyren-1-yl)carbonyl-aza-ENA thymidine, Aza-ENA-pyr (**Y**)], show that they can bind to complementary RNA more strongly than to the DNA. The Aze-pyr (**X**) containing ODNs with the complementary DNA and RNA duplexes showed an increase in the fluorescence intensity (measured at $\lambda_{em} \approx 376$ nm) depending upon the nearest neighbor at the 3′-end to **X** [dA (∼12−20-fold) > dG (∼9−20-fold) > dT (∼2.5−20-fold) > dC (∼6−13-fold)]. They give high fluorescence quantum yields ($\Phi_F = 0.13-0.89$) as compared to those of the single-stranded ODNs. The Aza-ENA-pyr (**Y**)-modified ODNs, on the other hand, showed an enhancement of the fluorescence intensity only with the complementary DNA (1.4−3.9-fold, $\Phi_F = 0.16-0.47$); a very small increase in fluorescence is also observed with the complementary RNA (1.1−1.7-fold, $\Phi_F = 0.17-0.22$), depending both upon the site of the **Y** modification introduced as well as on the chemical nature of the nucleobase adjacent to the modification site into the ODN. The fluorescence properties, thermal denaturation experiments, absorption, and circular dichroism (CD) studies with the **X**- and **Y**-modified ODNs in the form of matched homo- and heteroduplexes consistently suggested (i) that the orientation of the pyrene moiety is outside the helix of the nucleic acid duplexes containing a dT−d/rA base pair at the 3′-end of the modification site for both **X** and **Y** types of modifications, and (ii) that the microenvironment around the pyrene moiety in the ODN/DNA and ODN/RNA duplexes is dictated by the chemical nature of the conformational constraint in the sugar moiety, as well as by the nature of neighboring nucleobases. The pyrene fluorescence emission in both **X** and **Y** types of the conformationally restricted nucleotides is found to be sensitive to a mismatched base present in the target RNA: (i) The **X**-modified ODN showed a decrease (∼37-fold) in the fluorescence intensity (measured at $\lambda_{em} \approx 376$ nm) upon duplex formation with RNA containing a G nucleobase mismatch (dT−rG pair instead of dT−rA) opposite to the modification site. (ii) In contrast, the **Y**-modified ODN in the heteroduplex resulted in a ∼3-fold increase in the fluorescence intensity upon dT−rG mismatch, instead of matched dT−rA pair, in the RNA strand. Our data corroborate that the pyrene moiety is intercalated in the **X**-modified mismatched ODN/RNA (G mismatch) heteroduplex as compared to that of the **Y**-modified ODN/RNA (G mismatch) heteroduplex, in which it is located outside the helix.

1. Introduction

The fluorescence assays used in nucleic acid detection are either based on nonspecific double-stranded DNA (dsDNA) binding dyes, or on the fluorescently labeled oligonucleotide (ON) probes, which hybridize specifically to the target DNA or RNA by taking advantage of the Watson−Crick base-pairing

10.1021/jo702747w CCC: $40.75
Published on Web 03/11/2008

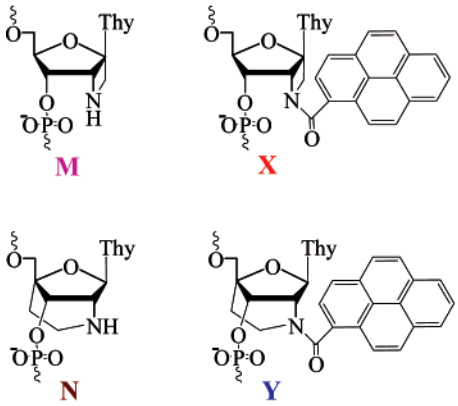

ODN 1 : 5'-dCTTCA**X**TTTTTCTTC
ODN 2 : 5'-dCTTCATT**X**TTTCTTC
ODN 3 : 5'-dCTTCATTTT**X**TCTTC
ODN 4 : 5'-dCTTCA**Y**TTTTTCTTC
ODN 5 : 5'-dCTTCATT**Y**TTTCTTC
ODN 6 : 5'-dCTTCATTTT**Y**TCTTC
ODN 7 : 5'-dCTTCA**X**CTTTTCTTC
ODN 8 : 5'-dCTTCA**X**ATTTTCTTC
ODN 9 : 5'-dCTTCA**X**GTTTTCTTC
ODN 10 : 5'-dCTTCG**X**GTTTTCTTC
ODN 11 : 5'-dCTTCA**Y**CTTTTCTTC
ODN 12 : 5'-dCTTCA**Y**ATTTTCTTC
ODN 13 : 5'-dCTTCA**Y**GTTTTCTTC
ODN 14 : 5'-dCTTCG**Y**GTTTTCTTC

FIGURE 1. Structures of azetidine thymidine [Azetidine (**M**)], 2′-*N*-(pyren-1-yl)carbonyl-azetidine thymidine [Aze-pyr (**X**)], aza-ENA thymidine [Aza-ENA (**N**)], and 2′-*N*-(pyren-1-yl)carbonyl-aza-ENA thymidine [Aza-ENA-pyr (**Y**)] monomers are shown. Modified oligodeoxynucleotide sequences (ODNs **1**−**14**) used in this study are also listed. For a complete list of oligonucleotides, see Table S1 in the Supporting Information.

rules. The nonspecific probes, such as ethidium bromide[1] or oxazole yellow dye (YO-PRO 1),[2] intercalate into double-stranded DNA with a dramatic increase in fluorescence and are capable of detecting amplification and product accumulation but are unable to provide unambiguous verification of the identity of the amplified product.[3] Specific detection of nucleic acids based on fluorescence increase upon hybridization to DNA or RNA of cyanine dyes conjugated to ONs[4,5] or peptide nucleic acids (PNAs)[6,7] has some disadvantages: (i) low fluorescence quantum yields of the hybridized duplexes,[5,6] (ii) sequence- and temperature-dependent high levels of fluorescence of the single-stranded probes,[4,6,8] and (iii) small increases in fluorescence intensity upon hybridization with complements.[5] Another type of approach based on the increase of the distance between fluorophore and neighboring nucleobases upon binding to a complementary ON has been used in such probes as molecular beacons,[9] TaqMan probes,[10,11] Scorpion primers,[12] or polyamide−fluorophore conjugates.[13] However, the sensitivity of assays with such probes may be limited by sequence-dependent nucleobase−fluorophore quenching.[13] Among several modifications, the pyrene-modified ONs have been synthesized and exploited as fluorescent probes of DNA and RNA in hybridization assays by utilizing the pyrene monomer[14−20] or excimer[21−26] fluorescence emission. The fact that pyrene fluorescence is largely affected by environmental factors, such as the nature of the solvent (fluorescence increases in the polar medium, whereas a fluorescence decrease is observed in the hydrophobic medium) or by the neighboring nucleobases (which often decrease fluorescence by quenching), gives possibility for one to employ its properties in the development of potential probes for the investigation of nucleic acid structures,[27−32] detection of single nucleotide polymorphisms,[17,19,33] or real-time PCR techniques.[34]

In this Article, we report on the synthesis and fluorescence properties of DNA probes containing novel sugar-conformation constrained 2′-*N*-pyrene-functionalized nucleosides [2′-*N*-(pyren-

(1) Higuchi, R.; Fockler, C.; Dollinger, G.; Watson, R. *Biotechnology* **1993**, *11*, 1026−1030.
(2) Ishiguro, T.; Saitoh, J.; Yawata, H.; Yamagishi, H.; Iwasaki, S.; Mitoma, Y. *Anal. Biochem.* **1995**, *229*, 207−213.
(3) Petty, J. T.; Bordelon, J. A.; Robertson, M. E. *J. Phys. Chem. B* **2000**, *104*, 7221−7227.
(4) Ishiguro, T.; Saitoh, J.; Yawata, H.; Otsuka, M.; Inoue, T.; Sugiura, Y. *Nucleic Acids Res.* **1996**, *24*, 4992−4997.
(5) Privat, E.; Melvin, T.; Merola, F.; Schweizer, G.; Prodhomme, S.; Asseline, U.; Vigny, P. *Photochem. Photobiol.* **2002**, *75*, 201−210.
(6) Svanvik, N.; Westman, G.; Wang, D.; Kubista, M. *Anal. Biochem.* **2000**, *281*, 26−35.
(7) Köhler, O.; Jarikote, D. V.; Seitz, O. *ChemBioChem* **2005**, *6*, 69−77.
(8) Svanvik, N.; Nygren, J.; Westman, G.; Kubista, M. *J. Am. Chem. Soc.* **2001**, *123*, 803−809.
(9) Tyagi, S.; Kramer, F. R. *Nat. Biotechnol.* **1996**, *14*, 303−308.
(10) Heid, C. A.; Stevens, J.; Livak, K. J.; Williams, P. M. *Genome Res.* **1996**, *6*, 986−994.
(11) Gelmini, S.; Orlando, C.; Sestini, R.; Vona, G.; Pinzani, P.; Ruocco, L.; Pazzagli, M. *Clin. Chem.* **1997**, *43*, 752−758.
(12) Whitcombe, D.; Theaker, J.; Guy, S. P.; Brown, T.; Little, S. *Nat. Biotechnol.* **1999**, *17*, 804−807.
(13) Rucker, V. C.; Foister, S.; Melander, C.; Dervan, P. B. *J. Am. Chem. Soc.* **2003**, *125*, 1195−1202.
(14) Yamana, K.; Iwase, R.; Furutani, S.; Tsuchida, H.; Zako, H.; Yamaoka, T.; Murakami, A. *Nucleic Acids Res.* **1999**, *27*, 2387−2392.
(15) Yamana, K.; Zako, H.; Asazuma, K.; Iwase, R.; Nakano, H.; Murakami, A. *Angew. Chem., Int. Ed.* **2001**, *40*, 1104−1106.
(16) Korshun, V. A.; Stetsenko, D. A.; Gait, M. J. *J. Chem. Soc., Perkin Trans. 1* **2002**, 1092−1104.
(17) Okamoto, A.; Kanatani, K.; Saito, I. *J. Am. Chem. Soc.* **2004**, *126*, 4820−4827.
(18) Nakamura, M.; Fukunaga, Y.; Sasa, K.; Ohtoshi, Y.; Kanaori, K.; Hayashi, H.; Nakano, H.; Yamana, K. *Nucleic Acids Res.* **2005**, *33*, 5887−5895.
(19) Dohno, C.; Saito, I. *ChemBioChem* **2005**, *6*, 1075−1081.
(20) Hrdlicka, P. J.; Babu, B. R.; Sorensen, M. D.; Harrit, N.; Wengel, J. *J. Am. Chem. Soc.* **2005**, *127*, 13293−13299.
(21) Lewis, F. D.; Zhang, Y.; Letsinger, R. L. *J. Am. Chem. Soc.* **1997**, *119*, 5451−5452.
(22) Paris, P. L.; Langenhan, J. M.; Kool, E. T. *Nucleic Acids Res.* **1998**, *26*, 3789−3793.
(23) Masuko, M.; Ohtani, H.; Ebata, K.; Shimadzu, A. *Nucleic Acids Res.* **1998**, *26*, 5409−5416.
(24) Okamoto, A.; Ichiba, T.; Saito, I. *J. Am. Chem. Soc.* **2004**, *126*, 8364−8365.
(25) Fujimoto, K.; Shimizu, H.; Inouye, M. *J. Org. Chem.* **2004**, *69*, 3271−3275.
(26) Yamana, K.; Fukunaga, Y.; Ohtani, Y.; Sato, S.; Nakamura, M.; Kim Won, J.; Akaike, T.; Maruyama, A. *Chem. Commun.* **2005**, 2509−2511.
(27) Bevilacqua, P. C.; Kierzek, R.; Johnson, K. A.; Turner, D. H. *Science* **1992**, *258*, 1355−1358.
(28) Kierzek, R.; Li, Y.; Turner, D. H.; Bevilacqua, P. C. *J. Am. Chem. Soc.* **1993**, *115*, 4985−4992.
(29) Silverman, S. K.; Cech, T. R. *Biochemistry* **1999**, *38*, 14224−14237.
(30) Kostenko, E.; Dobrikov, M.; Pyshnyi, D.; Petyuk, V.; Komarova, N.; Vlassov, V.; Zenkova, M. *Nucleic Acids Res.* **2001**, *29*, 3611−3620.
(31) Mahara, A.; Iwase, R.; Sakamoto, T.; Yamana, K.; Yamaoka, T.; Murakami, A. *Angew. Chem., Int. Ed.* **2002**, *41*, 3648−3650.
(32) Mahara, A.; Iwase, R.; Sakamoto, T.; Yamaoka, T.; Yamana, K.; Murakami, A. *Bioorg. Med. Chem.* **2003**, *11*, 2783−2790.

SCHEME 1 [a,b]

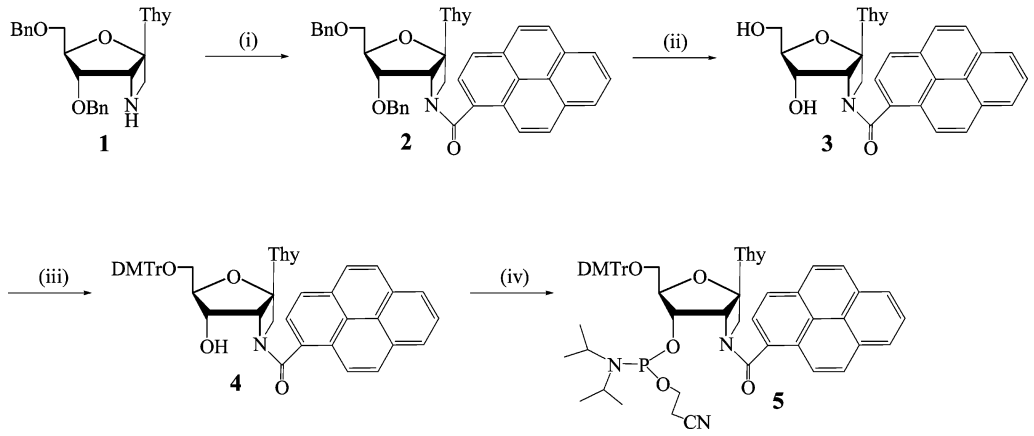

[a] Reagents and conditions: (i) pyrenecarboxylic acid, PyBOP, DIPEA, DMF, rt, 1.5 h, 87%; (ii) ammonium formate, 20% $Pd(OH)_2$/C, methanol, reflux, 36 h, 78%; (iii) DMTrCl, pyridine, rt, 12 h, 82%; (iv) $NC(CH_2)_2OP(Cl)N(^iPr)_2$, DIPEA, THF, 0 °C, 30 min, then rt, 1.5 h, 85%. [b] Abbreviations: Thy, thymin-1-yl, Bn, Benzyl; DMTr, 4,4′-dimethoxytrityl; PyBOP, (benzotriazol-1-yloxy)tripyrrolidinophosphonium hexafluorophosphate; DIPEA, diisopropylethylamine; DMF, *N*,*N*-dimethylformamide; rt, room temperature; THF, tetrahydrofuran.

SCHEME 2 [a]

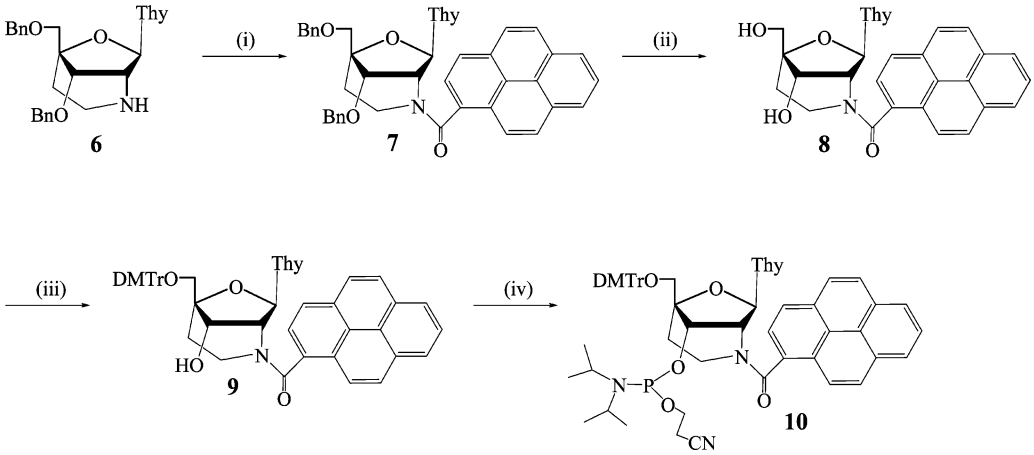

[a] Reagents and conditions: (i) pyrenecarboxylic acid, PyBOP, DIPEA, DMF, rt, 2 h, 90%; (ii) ammonium formate, 20% $Pd(OH)_2$/C, methanol, reflux, 36 h, 82%; (iii) DMTrCl, pyridine, rt, 32 h, 76%; (iv) $NC(CH_2)_2OP(Cl)N(^iPr)_2$, DIPEA, THF, 0 °C, 30 min, then rt, overnight, 73%.

1-yl)carbonyl-azetidine thymidine, Aze-pyr (**X**), and 2′-*N*-(pyren-1-yl)carbonyl-aza-ENA thymidine, Aza-ENA-pyr (**Y**) in Figure 1]. It has been found that the chemical structure of different conformationally constrained units (Azetidine[35] vs Aza-ENA[36]) on the sugar moiety imparts different fluorescence properties of *N*-conjugated pyren-1-yl moiety in the ODNs/DNA versus ODNs/RNA duplexes. Unlike previously reported DNA probes containing 2′-*N*-(pyren-1-yl)carbonyl-2′-amino-LNA modification,[20] the **X**-modified ODNs showed DNA/RNA complements discrimination depending on the sequence context with high fluorescence quantum yields ($\Phi_F = 0.13-0.89$). Also, in contrast to the 2′-*O*-(1-pyrenylmethyl)uridine[14,15] or 2′-*O*-(pyren-1-ylmethylcarbamoyl)uridine[16]-modified ONs, which display significant fluorescence increase upon hybridization with RNA, the **Y**-modified probes show an enhancement of the fluorescence intensity only with the complementary DNA. The Aze-pyr (**X**) versus Aza-ENA-pyr (**Y**) can successfully distinguish between the matched nucleobase, A, and the mismatched nucleobase, G, in the complementary RNA. Thus, this constitutes the example of RNA base-mismatch recognition (dT−rA vs dT−rG pair) by fluorescence emission using pyrene-modified DNA in the DNA/RNA heteroduplex. It is noteworthy that earlier mismatch discrimination studies have been performed in pyrene-modified DNA/DNA[17,19,26] or RNA/RNA[15] homoduplexes. Only 2′-*N*-(pyren-1-yl)acetyl-2′-amino-α-L-LNA probes[37] have been recently used for detection of single nucleotide mismatches in DNA/RNA heteroduplex, however, utilizing the mismatch detection mechanism based on differences in fluorescence intensity between duplexes with matched or mismatched targets upon excimer formation.

2. Results

2.1. Synthesis of Pyrene-Modified ODNs. Synthesis of the novel Aze-pyr (**X**) and Aza-ENA-pyr (**Y**) nucleosides is shown in Schemes 1 and 2. Nucleosides **1** and **6** were prepared

(33) Nakatani, K. *ChemBioChem* **2004**, *5*, 1623−1633.
(34) Wilhelm, J.; Pingoud, A. *ChemBioChem* **2003**, *4*, 1120−1128.
(35) Honcharenko, D.; Varghese, O. P.; Plashkevych, O.; Barman, J.; Chattopadhyaya, J. *J. Org. Chem.* **2006**, *71*, 299−314.
(36) Varghese, O. P.; Barman, J.; Pathmasiri, W.; Plashkevych, O.; Honcharenko, D.; Chattopadhyaya, J. *J. Am. Chem. Soc.* **2006**, *128*, 15173−15187.
(37) Kumar, T. S.; Wengel, J.; Hrdlicka, P. J. *ChemBioChem* **2007**, *8*, 1122−1125.

TABLE 1. Thermal Denaturation Studies[a] of Modified ODNs in Duplexes with Complementary DNA and RNA

			T_m/°C	
no.	ODNs[b]	ODN sequences	duplex with complementary DNA **2**[c]	duplex with complementary RNA **1**[d]
1	DNA **1** (native)	5′-dCTTCATTTTTTCTTC	43.5	43
2	ODN **1** (Aze-pyr)	5′-dCTTCA**X**TTTTTCTTC	32.5	37.5
3	ODN **2** (Aze-pyr)	5′-dCTTCATT**X**TTTCTTC	31	38
4	ODN **3** (Aze-pyr)	5′-dCTTCATTTT**X**TCTTC	30.5	37
5	ODN **4** (Aza-ENA-pyr)	5′-dCTTCA**Y**TTTTTCTTC	34	42
6	ODN **5** (Aza-ENA-pyr)	5′-dCTTCATT**Y**TTTCTTC	34	40.5
7	ODN **6** (Aza-ENA-pyr)	5′-dCTTCATTTT**Y**TCTTC	34	40
8	ODN **1a** (Azetidine)	5′-dCTTCA**M**TTTTTCTTC	41[e]	40[e]
9	ODN **2a** (Azetidine)	5′-dCTTCATT**M**TTTCTTC	39[e]	40[e]
10	ODN **3a** (Azetidine)	5′-dCTTCATTTT**M**TCTTC	39.5[e]	40[e]
11	ODN **1b** (Aza-ENA)	5′-dCTTCA**N**TTTTTCTTC	42[e]	48[e]
12	ODN **2b** (Aza-ENA)	5′-dCTTCATT**N**TTTCTTC	42[e]	47.5[e]
13	ODN **3b** (Aza-ENA)	5′-dCTTCATTTT**N**TCTTC	42.5[e]	46.5[e]

[a] T_m values measured as the maximum of the first derivative of the melting curve (A_{260} vs temperature) recorded in medium salt buffer ($[Na^+] = 110$ mM, $[Cl^-] = 100$ mM, pH 7.0 (NaH_2PO_4/Na_2HPO_4)), using 1.0 μM concentrations of the two complementary strands. [b] See Figure 1 for all abbreviations. [c] DNA **2**: 5′-dGAAGAAAAAATGAAG. [d] RNA **1**: 5′-rGAAGAAAAAAUGAAG. [e] T_m's were taken from ref 39, where T_m's of the corresponding native DNA **1**/DNA **2** and DNA **1**/RNA **1** were found to be 45 and 44 °C, respectively.

according to the literature methods.[35,36] Appropriately pyrene-functionalized units **2** and **7** were synthesized via coupling of pyrenecarboxylic acid[24] with corresponding nucleosides **1** and **6**. In both cases, the reaction afforded a mixture of rotamers (87% and 90%, respectively) because of the restricted rotation of the amide bond of the (pyren-1-yl)carbonyl unit. Fully deprotected nucleosides **3** (78%) and **8** (82%) were prepared by debenzylation of corresponding derivatives **2** and **7**, respectively, using $Pd(OH)_2$/ammonium formate in methanol. Treatment of unprotected nucleosides **3** and **8** with 4,4′-dimethoxytrityl chloride in pyridine afforded **4** and **9** in 82% and 76%, respectively, which were transformed to their corresponding phosphoramidites **5** (85%) and **10** (73%) for solid-phase oligonucleotide synthesis.

ODNs **1**−**14** containing **X** and **Y** monomers (Figure 1) were synthesized according to conventional DNA synthesis[38] except for extended coupling time for phosphoramidites **5** [10 min, 4,5-dicarbonitrile-1*H*-imidazole (DCI) as an activator] and **10** [10 min, 5-(ethylthio)-1*H*-tetrazole (ETT) as an activator]. ODNs were deprotected using 32% aqueous ammonia at room temperature during 24 h, purified by polyacrylamide gel electrophoresis (PAGE), and their composition was verified by MALDI-TOF MS analysis [Table S1 in the Supporting Information]. Single modifications (monomers **X** or **Y**) were placed one at a time at three different positions in the central part of the non-self-complementary oligodeoxynucleotide 15-mers with the same nucleobase context at the 3′-end of the modification site (Figure 1, ODNs **1**−**6**) as well as with different nucleobase neighbors at both sides (Figure 1, ODNs **1**, **4**, **7**−**14**).

2.2. Thermal Denaturation Studies of Pyrene-Modified ODNs. The binding of pyrene-modified ODNs **1**−**6** containing monomers **X** or **Y** to their complementary DNA **2** and RNA **1** was investigated by UV thermal denaturation experiments in medium salt neutral buffer, and compared to the corresponding unmodified native, Azetidine[35] (**M**)-, and Aza-ENA[36,39] (**N**)-modified duplexes. In all cases, melting profiles at 260 nm displayed sigmoidal curves with a shape similar to those for the corresponding unmodified duplexes. The binding properties for both **X**-modified ODNs **1**−**3** and **Y**-modified ODNs **4**−**6** are summarized in Table 1.

The **X**-modified ODNs **1**−**3**/RNA hybrid duplexes (entries 2−4 in Table 1) were found to be less stable by 2−3 °C than the corresponding Azetidine-modified ODNs/RNA duplexes[35] (entries 8−10 in Table 1); they also have a 5−6 °C drop in melting temperatures (T_m's) as compared to the native counterpart. The duplexes of **Y**-modified ODNs **4**−**6** with complementary RNA (entries 5−7 in Table 1) showed relatively higher target binding affinity ($\Delta T_m = +2.5$ to $+4.5$ °C) as compared to the isosequential **X**-modified ODNs **1**−**3**/RNA hybrids (entries 2−4 in Table 1). However, incorporation of the pyren-1-yl moiety to the Aza-ENA unit leads to a ∼5−6 °C drop in T_m with respect to the corresponding Aza-ENA-modified ODNs/RNA hybrid duplexes[36] (entries 11−13 in Table 1) and ∼1−3 °C drop as compared to the native counterpart. With complementary DNA **2**, all pyrene-modified ODNs showed a significant drop in duplex melting with respect to the native counterpart and a similar destabilizing effect of pyren-1-yl moiety ($\Delta T_m = -6$ to -7 °C) as compared to the corresponding isosequential **M**- and **N**-modified duplexes.

Binding affinity of pyrene-modified ODNs **1** and **4** (entries 2−4 for **X** and entries 6−8 for **Y** in Table 2) to the RNA possessing a single base mismatch (RNAs **2**−**4**, Table 1 in Supporting Information) appeared to be quite similar to the T_m profile of the ODNs/DNA **2** duplexes.

2.3. Absorption Spectra of the Pyrene-Modified ODNs and Their Duplexes with DNA and RNA. The pyrene absorption maxima were found to be at 341 nm for both Aze-pyr (**X**)-modified nucleoside **3** and Aza-ENA-pyr (**Y**) nucleoside **8** (Schemes 1 and 2) in sodium phosphate buffer (pH 7.0) (Figure S1 in the Supporting Information), which is characteristic for the pyrene chromophore. Figure 2 shows, as an example, the absorption spectra of two isosequential (i) **X**-modified ODN **1**, its duplexes with complementary DNA **2** and RNA **1** (inset A in Figure 2), and (ii) **Y**-modified ODN **4** and its corresponding DNA **2** and RNA **1** duplexes (inset B in Figure 2) in the region between 300 and 400 nm.

For the **X**-modified ODN **1**, the pyrene absorption band at 347 nm was found to be shifted to a shorter wavelength upon duplex formation with the complementary DNA **2** (343 nm) or

(38) Caruthers, M. H.; Barone, A. D.; Beaucage, S. L.; Dodds, D. R.; Fisher, E. F.; McBride, L. J.; Matteucci, M.; Stabinsky, Z.; Tang, J. Y. *Methods Enzymol.* **1987**, *154*, 287−313.

(39) Honcharenko, D.; Barman, J.; Varghese, O. P.; Chattopadhyaya, J. *Biochemistry* **2007**, *46*, 5635−5646.

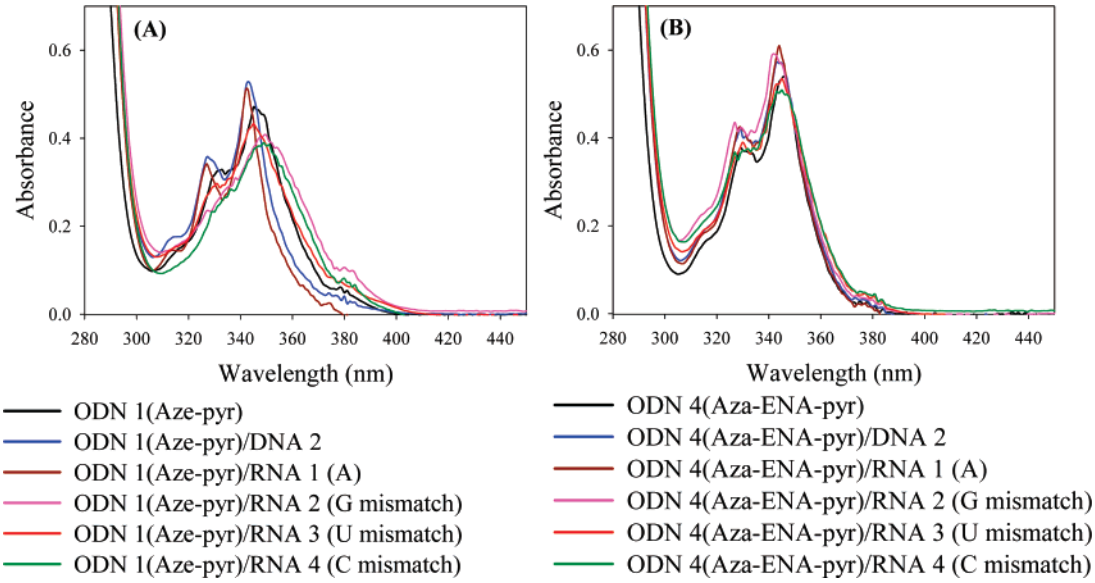

FIGURE 2. Absorption spectra of (A) Aze-pyr (**X**)-modified ODN **1** and (B) Aza-ENA-pyr (**Y**)-modified ODN **4** hybridized to the complementary DNA **2**, complementary RNA **1**, and single base mismatch (**G**, **U**, **C**) RNA **2**, RNA **3**, and RNA **4**, respectively. Spectra were recorded at a total strand concentration of 19.5 μM at 25 °C.

TABLE 2. Thermal Denaturation Studies[a] of Modified ODNs in Duplexes with RNA Possessing a Single Base Mismatch

no.	ODNs[b]	ODN sequences	T_m/°C duplex with mismatched RNA
1	ODN **1** (Aze-pyr)	5′-dCTTCA**X**TTTTTCTTC	37.5[c]
2	ODN **1** (Aze-pyr)	5′-dCTTCA**X**TTTTTCTTC	33.5[d]
3	ODN **1** (Aze-pyr)	5′-dCTTCA**X**TTTTTCTTC	33[e]
4	ODN **1** (Aze-pyr)	5′-dCTTCA**X**TTTTTCTTC	31[f]
5	ODN **4** (Aza-ENA-pyr)	5′-dCTTCA**Y**TTTTTCTTC	42[c]
6	ODN **4** (Aza-ENA-pyr)	5′-dCTTCA**Y**TTTTTCTTC	34[d]
7	ODN **4** (Aza-ENA-pyr)	5′-dCTTCA**Y**TTTTTCTTC	32[e]
8	ODN **4** (Aza-ENA-pyr)	5′-dCTTCA**Y**TTTTTCTTC	30.5[f]

[a] T_m values measured as the maximum of the first derivative of the melting curve (A_{260} vs temperature) recorded in medium salt buffer ([Na^+] = 110 mM, [Cl^-] = 100 mM, pH 7.0 (NaH_2PO_4/Na_2HPO_4)), using 1.0 μM concentrations of ODN and target RNA. [b] See Figure 1 for all abbreviations. [c] RNA = RNA **1**: 5′-rGAAGAAAAAAUGAAG. [d] RNA = RNA **2**: 5′-rGAAGAAAAA**G**UGAAG. [e] RNA = RNA **3**: 5′-rGAAGAAAAA**U**UGAAG. [f] RNA = RNA **4**: 5′-rGAAGAAAAA**C**UGAAG, the mismatch bases in RNA sequences are indicated by the bold and underline fonts.

RNA **1** (342 nm), which were close to the absorption maximum observed for the corresponding Aze-pyr-modified nucleoside **3**. However, the pyrene absorption band at 345 nm for the **Y**-modified ODN **4** showed very small changes (344 nm) in the corresponding DNA **2** or RNA **1** duplexes, as compared to the 341 nm for the corresponding Aza-ENA-pyr-modified nucleoside **8**. The difference in UV spectra between **X**-modified ODN **1** and **Y**-modified ODN **4** suggests that incorporation of either **X** or **Y** modification into oligonucleotide with the identical sequence motif changes the structure of the corresponding duplexes differently, which also changes the environment around the pyrene moiety in a different manner. Conformationally preorganized *North-East* (Azetidine, 44° < P < 54°, 29° < ϕ_m < 33°)[35] or *North* (Aza-ENA, 7° < P < 27°, 44° < ϕ_m < 52°)[36] (**M** and **N** in Figure 1) should have significant contribution in the location and interaction of the pyren-1-yl moiety in the ODN **1** or ODN **4**. It has been shown that the type of conformational constrains in the sugar moiety has varied influence on the molecular properties of the modified nucleosides (including the pK_a of the nucleobase)[40] depending on whether the modified sugar ring is a bicyclic 1′,2′-fused[35] or a 2′,4′-fused.[36] High amplitude and range of dynamics of the important backbone torsion (δ) in Azetidine versus Aza-ENA indicate that 1′,2′-fused nucleosides have higher flexibility of the backbone as compared to that of the 2′,4′-fused counterpart.[40] A small shift in pyrene maximum for the **X**-modified ODN **1**/RNA **1** hybrid with respect to the ODN **1**/DNA **2** duplex also indicates some differences in microenvironment around the pyrene unit. In contrast, these changes were not observed in case of **Y**-modified duplexes upon hybridization with the complementary DNA **2** or RNA **1**. Figure 2 also shows the absorption spectra profile for the **X**-modified ODN **1** and **Y**-modified ODN **4** hybridized with RNAs **2**, **3**, and **4** containing single base mismatch (G, U, C, respectively) opposite to the modification site in ODN strand. As for the hybrid duplex formed by **X**-modified ODN **1** and RNA **2** (G mismatch) as well as for **Y**-modified ODN **4**/RNA **2** (G mismatch) duplex, UV spectra showed uniquely different profiles. In the Aze-pyr-modified ODN **1**/RNA **2** (G mismatch) duplex, pyrene absorption band showed a red shift from 347 to 351 nm, whereas for the Aza-ENA-pyr-modified ODN **4**/RNA **2** (G mismatch) duplex, pyrene maximum shifted to the shorter wavelength, from 345 to 342 nm. In **X**-modified ODN **1**/RNA **4** (C mismatch) duplex, pyrene absorption band had a red shift of 2 nm. Other ODN **4**/RNA **3** (U mismatch), ODN **4**/RNA **4** (C mismatch), and ODN **1**/RNA **3** (U mismatch) showed the same wavelength of 344 nm for the pyrene absorption band.

2.4. Fluorescence Properties of Pyrene-Modified ODNs and Their Duplexes with DNA and RNA. Figure 3 shows the fluorescence emission spectra of Aze-pyr (**X**)-modified ODN **1** (inset A in Figure 3) and Aza-ENA-pyr (**Y**)-modified ODN **4** (inset B in Figure 3) and their corresponding duplexes with complementary DNA **2** or RNA **1** targets. Single-stranded ODN **1** containing **X** modification (Figure 1) exhibits an unstructured band at $\lambda_{max} \approx 412$ nm (inset A in Figure 3). Upon hybridization

(40) Plashkevych, O.; Chatterjee, S.; Honcharenko, D.; Pathmasiri, W.; Chattopadhyaya, J. *J. Org. Chem.* **2007**, *72*, 4716−4726.

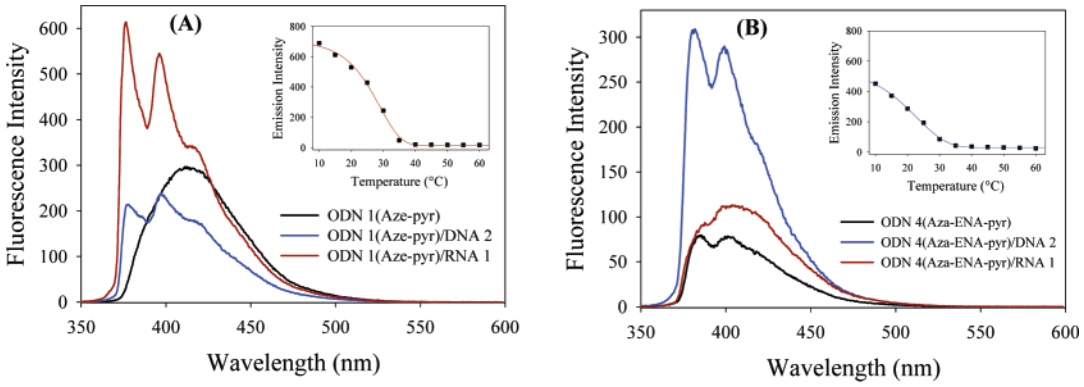

FIGURE 3. Fluorescence emission spectra of (A) Aze-pyr (**X**)-modified ODN **1** and (B) Aza-ENA-pyr (**Y**)-modified ODN **4** and the corresponding duplexes with complementary DNA **2** or RNA **1** targets. The temperature-dependent fluorescence changes (A) at 376 nm for the **X**-modified ODN **1**/RNA **1** duplex and (B) at 385 nm for the **Y**-modified ODN **4**/DNA **2** duplex are shown in the inset. Spectra were recorded at a total strand concentration of 0.8 μM and with an excitation wavelength of 340 nm.

of ODN **1** with complementary DNA **2** or RNA **1**, two vibronic bands appear at $\lambda_{max} \approx 376$ nm (band I) and $\lambda_{max} \approx 396$ nm (band III). Interestingly, fluorescence intensity (measured at $\lambda_{em} \approx 376$ nm) increased 18.5-fold in ODN **1**/RNA **1** hybrid and only 6.4-fold in ODN **1**/DNA **2** duplex (inset A in Figure 3). Other **X**-modified ODNs **2** and **3**, which have the same sequence motif at the 3′-end of the modification site, exhibited similar fluorescence properties (inset A in Figures S2 and S3 in the Supporting Information).

Introduction of **Y** modification into the isosequential ODN **4** (Figure 1) resulted in remarkably different fluorescence properties. Single-stranded ODN **4** displays structure involving two bands at $\lambda_{max} \approx 385$ nm and $\lambda_{max} \approx 399$ nm (inset B in Figure 3). The **Y**-modified ODN **4**/RNA **1** duplex showed similar but less structured shape with the same λ_{max} for bands I and III without significant changes in the fluorescence intensity (measured at $\lambda_{em} \approx 385$ nm). In contrast, a 3.9-fold increase in fluorescence intensity and formation of two vibronic bands at $\lambda_{max} \approx 382$ nm (band I) and $\lambda_{max} \approx 399$ nm (band III) resulted upon duplex formation with complementary DNA **2** (inset B in Figure 3). However, other **Y**-modified ODNs **5** and **6** containing dT at the 3′-end of the modification site did not show a significant difference in fluorescence intensity upon hybridization with complementary DNA **2** or RNA **1** (inset B in Figures S2 and S3 in the Supporting Information).

Fluorescence quantum yields (Φ_F) of the single-stranded probes containing **X** or **Y** modifications and their corresponding duplexes with DNA or RNA were measured[41] in sodium phosphate buffer (pH 7.0) at 20 °C relative to the pyrenebutanoic acid (PBA) in methanol ($\Phi_F = 0.065$)[42,43] (see Experimental Section). The quantum yields of fully deprotected Aze-pyr nucleoside **3** and Aza-ENA-pyr nucleoside **8** (Schemes 1 and 2) were determined to be $\Phi_F = 0.83$ and $\Phi_F = 0.28$, respectively (Figures S4 and S5 in the Supporting Information). ODNs **1**−**6** containing modification at different positions in the sequence with the same nucleotide sequence at the 3′-end of the modification site showed different fluorescence properties depending on the type of modification. Duplexes of **X**-modified ODNs **1**−**3** (Figure 1) with complementary RNA **1** exhibit the same high fluorescence quantum yields ($\Phi_F = 0.80-0.85$) (entries 3, 9, and 12 in Table 3) as the corresponding unprotected nucleoside **3**, showing higher quantum yields as compared to the state-of-the-art pyrene-labeled probes,[17,19] and were found to be comparable to Φ_F of probes containing pyrene-functionalized 2′-amino-LNA.[20] **X**-modified ODNs **1**−**3**/DNA **2** homoduplexes display a decrease in fluorescence ($\Phi_F = 0.36-0.40$) (Table 3). However, fluorescence of duplexes formed by **Y**-modified ODNs **4**−**6** (Figure 1) with complementary DNA **2** or RNA **1** ($\Phi_F = 0.19-0.22$) did not change much as compared to the corresponding single-stranded probes ($\Phi_F = 0.16-0.17$), except the homoduplex of **Y**-modified ODN **4** with DNA **2**, which showed an enhancement of fluorescence quantum yield ($\Phi_F = 0.47$) (Table 3), probably related to the site-dependency of incorporation of Aza-ENA-pyr modification to the ODN.

The emission intensities at $\lambda_{em} \approx 376$ nm for the **X**-modified ODN **1**/RNA (inset A in Figure 3) or at $\lambda_{em} \approx 382$ nm for the **Y**-modified ODN **4**/DNA **2** (inset B in Figure 3) duplexes were decreased with melting of the corresponding duplexes (Figures S6 and S7 in the Supporting Information), and only the emissions for the corresponding modified ODN **1** or ODN **4** were observed at high temperature. However, a 2-fold decrease in intensity for the pyrene monomer emission does not correspond to the melting T_m of the duplex in both cases (Table 1). The T_m-like curve shows a pseudomelting behavior approximately ∼10−14 °C lower than the actual melting observed at 260 nm (UV). This suggests that the pyren-1-yl moiety does not contribute in the duplex stabilization through stacking or/and Watson−Crick hydrogen bonding; its temperature-dependent fluorescence changes, on the other hand, suggest that its exposure to the immediate microenvironment changes in a systematic manner during melting of the duplex.

Aze-pyr (**X**)-modified ODNs containing dC or dA at the 3′-end of the modification site in duplexes with complementary DNA or RNA display high fluorescence quantum yields up to 0.59 or 0.89, respectively (ODNs **7** and **8** in Table 3, Figure S8 in the Supporting Information), without discrimination between DNA and RNA. The **X**-modified ODNs containing dG only at the 3′-end of the modification site only, or at both 3′- and 5′-ends of the **X** modification in ODN/DNA or ODN/RNA duplexes, showed relatively poorer fluorescence quantum yields ($\Phi_F = 0.13-0.21$) (ODNs **9** and **10** in Table 3, Figure S9 in the Supporting Information). However, Aza-ENA-pyr (**Y**)-

(41) Fery-Forgues, S.; Lavabre, D. *J. Chem. Educ.* **1999**, *76*, 1260−1264.
(42) Manoharan, M.; Tivel, K. L.; Zhao, M.; Nafisi, K.; Netzel, T. L. *J. Phys. Chem.* **1995**, *99*, 17461−17472.
(43) Netzel, T. L.; Nafisi, K.; Headrick, J.; Eaton, B. E. *J. Phys. Chem.* **1995**, *99*, 17948−17955.

TABLE 3. Relative Fluorescence Emission Intensities and Fluorescence Quantum Yields for the Single-Stranded Pyrene-Modified ODNs and Their Duplexes with DNA or RNA

no.	ODNs[a]	single-stranded ODNs and duplexes with complementary DNA or RNA[b]	relative fluorescence intensity[c] (λ_{max}) 378 nm (band I)	391 nm (band III)	ratio of intensity (band III/band I)	Fluorescent Φ
1	ODN **1**	5′-dCTTCA**X**TTTTTCTTC	1.0[d]	7.0[e]	7.0	0.63
2	(Aze-pyr)	5′-dCTTCA**X**TTTTTCTTC−DNA **2**	6.4[d]	7.1[e]	1.1	0.40
3		5′-dCTTCA**X**TTTTTCTTC−RNA **1**	18.5[d]	16.5[e]	0.9	0.83
4		5′-dCTTCA**X**TTTTTCTTC−RNA **2** (G mismatch)	0.5[d]	2.0[e]	4.0	0.21
5		5′-dCTTCA**X**TTTTTCTTC−RNA **3** (U mismatch)	4.0[d]	8.2[e]	2.0	0.75
6		5′-dCTTCA**X**TTTTTCTTC−RNA **4** (C mismatch)	0.9[d]	5.1[e]	5.7	0.79
7	ODN **2**	5′-dCTTCATT**X**TTTCTTC	1.0[d]	10.5[f]	10.5	0.69
8	(Aze-pyr)	5′-dCTTCATT**X**TTTCTTC−DNA **2**	5.3[d]	7.8[f]	1.5	0.39
9		5′-dCTTCATT**X**TTTCTTC−RNA **1**	19.9[d]	19.5[f]	1.0	0.85
10	ODN **3**	5′-dCTTCATTTT**X**TCTTC	1.0	5.0[f]	5.0	0.60
11	(Aze-pyr)	5′-dCTTCATTTT**X**TCTTC−DNA **2**	2.7	4.1[f]	1.5	0.36
12		5′-dCTTCATTTT**X**TCTTC−RNA **1**	8.8	10.6[f]	1.2	0.80
13	ODN **4**	5′-dCTTCA**Y**TTTTTCTTC	1.0[g]	1.0[h]	1.0	0.16
14	(Aza-ENA-pyr)	5′-dCTTCA**Y**TTTTTCTTC−DNA **2**	3.9[g]	3.7[h]	0.9	0.47
15		5′-dCTTCA**Y**TTTTTCTTC−RNA **1**	1.1[g]	1.4[h]	1.3	0.19
16		5′-dCTTCA**Y**TTTTTCTTC−RNA **2** (G mismatch)	3.0[g]	2.6[h]	0.9	0.27
17		5′-dCTTCA**Y**TTTTTCTTC−RNA **3** (U mismatch)	1.9[g]	2.2[h]	1.2	0.34
18		5′-dCTTCA**Y**TTTTTCTTC−RNA 4 (C mismatch)	2.3[g]	2.6[h]	1.1	0.43
19	ODN **5**	5′-dCTTCATT**Y**TTTCTTC	1.0[g]	1.0[h]	1.0	0.16
20	(Aza-ENA-pyr)	5′-dCTTCATT**Y**TTTCTTC−DNA **2**	1.4[g]	1.5[h]	1.1	0.21
21		5′-dCTTCATT**Y**TTTCTTC−RNA **1**	1.3[g]	1.5[h]	1.2	0.21
22	ODN **6**	5′-dCTTCATTTT**Y**TCTTC	1.0[g]	1.0[h]	1.0	0.17
23	(Aza-ENA-pyr)	5′-dCTTCATTTT**Y**TCTTC−DNA **2**	1.4[g]	1.6[h]	1.1	0.21
24		5′-dCTTCATTTT**Y**TCTTC−RNA **1**	1.4[g]	1.7[h]	1.2	0.22
25	ODN **7**	5′-dCTTCA**X**CTTTTCTTC	1.0[d]	5.4[e]	5.4	0.53
26	(Aze-pyr)	5′-dCTTCA**X**CTTTTCTTC−DNA **3**	13.6[d]	11.9[e]	0.9	0.59
27		5′-dCTTCA**X**CTTTTCTTC−RNA **5**	5.7[d]	8.3[e]	1.5	0.57
28	ODN **8**	5′-dCTTCA**X**ATTTTCTTC	1.0[d]	8.7[e]	8.7	0.73
29	(Aze-pyr)	5′-dCTTCA**X**ATTTTCTTC−DNA **4**	12.3[d]	13.9[e]	1.1	0.85
30		5′-dCTTCA**X**ATTTTCTTC−RNA **6**	20.2[d]	18.8[e]	0.9	0.89
31	ODN **9**	5′-dCTTCA**X**GTTTTCTTC	1.0[d]	4.0[e]	4.0	0.08
32	(Aze-pyr)	5′-dCTTCA**X**GTTTTCTTC−DNA **5**	19.7[d]	17.7[e]	0.9	0.19
33		5′-dCTTCA**X**GTTTTCTTC−RNA **7**	9.2[d]	10.0[e]	1.1	0.13
34	ODN **10**	5′-dCTTCG**X**GTTTTCTTC	1.0[d]	3.8[e]	3.8	0.06
35	(Aze-pyr)	5′-dCTTCG**X**GTTTTCTTC−DNA **6**	26.1[d]	23.6[e]	0.9	0.21
36		5′-dCTTCG**X**GTTTTCTTC−RNA **8**	23.3[d]	21.6[e]	0.9	0.18
37	ODN **11**	5′-dCTTCA**Y**CTTTTCTTC	1.0[g]	1.0[h]	1.0	0.13
38	(Aza-ENA-pyr)	5′-dCTTCA**Y**CTTTTCTTC−DNA **3**	1.5[g]	1.7[h]	1.1	0.25
39		5′-dCTTCA**Y**CTTTTCTTC−RNA **5**	1.2[g]	1.2[h]	1.0	0.17
40	ODN **12**	5′-dCTTCA**Y**ATTTTCTTC	1.0[g]	1.0[h]	1.0	0.33
41	(Aza-ENA-pyr)	5′-dCTTCA**Y**ATTTTCTTC−DNA **4**	0.7[g]	0.8[h]	1.1	0.21
42		5′-dCTTCA**Y**ATTTTCTTC−RNA **6**	0.7[g]	0.8[h]	1.1	0.22
43	ODN **13**	5′-dCTTCA**Y**GTTTTCTTC	1.0[g]	0.8[h]	0.8	0.06
44	(Aza-ENA-pyr)	5′-dCTTCA**Y**GTTTTCTTC−DNA **5**	3.0[g]	3.4[h]	1.1	0.16
45		5′-dCTTCA**Y**GTTTTCTTC−RNA **7**	1.6[g]	1.6[h]	1.0	0.10
46	ODN **14**	5′-dCTTCG**Y**GTTTTCTTC	1.0[g]	0.8[h]	0.8	0.04
47	(Aza-ENA-pyr)	5′-dCTTCG**Y**GTTTTCTTC−DNA **6**	2.7[g]	3.0[h]	1.1	0.16
48		5′-dCTTCG**Y**GTTTTCTTC−RNA **8**	1.7[g]	1.7[h]	1.0	0.09

[a] See Figure 1 for all abbreviations. [b] DNA **2**: 5′-dGAAGAAAAAATGAAG. DNA **3**: 5′-dGAAGAAAAGATGAAG. DNA **4**: 5′-dGAAGAAAATATGAAG. DNA **5**: 5′-dGAAGAAAACATGAAG. DNA **6**: 5′-dGAAGAAAACACGAAG. RNA **1**: 5′-rGAAGAAAAAAUGAAG. RNA **2**: 5′-rGAAGAAAAA**G**UGAAG. RNA **3**: 5′-rGAAGAAAAA**U**UGAAG. RNA **4**: 5′-rGAAGAAAAA**C**UGAAG. RNA **5**: 5′-rGAAGAAAAGAUGAAG. RNA **6**: 5′-rGAAGĀAAAUAUGAAG. RNA **7**: 5′-rGAAGAĀAACAUGAAG. RNA **8**: 5′-rGAAGAAĀACACGAAG. [c] Relative fluorescence intensities were obtained at 20 °C based on the single-stranded ODNs **1**−**6**. [d] Measured at λ_{max} 376 nm (band I). [e] Measured at λ_{max} 396 nm (band III). [f] Measured at λ_{max} 397 nm (band III). [g] Measured at λ_{max} 385 nm (band I). [h] Measured at λ_{max} 399 nm (band III).

modified ODNs **11**, **13**, and **14** with different nucleobase adjacent to the modification site, upon hybridization with complementary DNA or RNA, reveal fluorescence ($\Phi_F = 0.09-0.25$, Table 3, inset A in Figure S10, and Figure S11 in the Supporting Information) similar to that of **Y**-modified ODNs **4**−**6**. The **Y**-modified ODN **12**/DNA **4** and ODN **12**/RNA **6** duplexes showed a small decrease in fluorescence as compared to the single-strand ODN **12** containing dA at the 3′-end of the modification site (Table 3, inset B in Figure S10 in the Supporting Information).

In Table 3 are shown the relative fluorescence emission intensities (bands I and III) for the single-stranded modified ODNs and their duplexes with DNA or RNA. The modulation of intensity of these two pyrene bands as a function of their exposure to the microenvironment is well known,[44,45] when pyrene-1-yl chromophore is acting as a reporter group for the polarity changes in the microenvironment. The incorporation of different pyrene-modified units into isosequential ODNs resulted in different fluorescence intensity ratios of band III/band I for the corresponding Aze-pyr (**X**)-modified ODN **1**

(44) Nakajima, A. *Bull. Chem. Soc. Jpn.* **1971**, *44*, 3272−3277.
(45) Kalyanasundaram, K.; Thomas, J. K. *J. Am. Chem. Soc.* **1977**, *99*, 2039−2044.

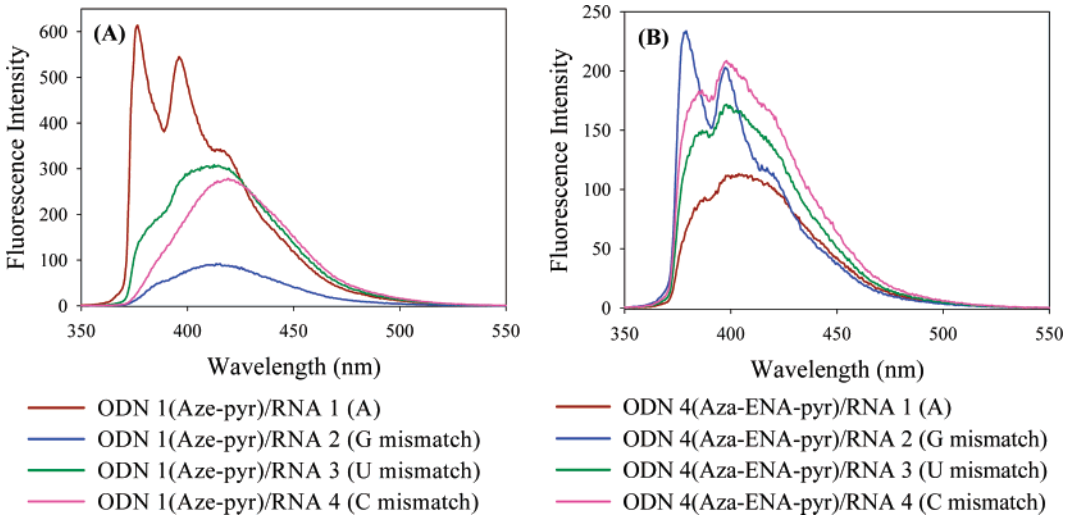

FIGURE 4. Fluorescence emission spectra of (A) Aze-pyr (**X**)-modified ODN **1** and (B) Aza-ENA-pyr (**Y**)-modified ODN **4** hybridized to the complementary RNA **1** and single base mismatch (**G**, **U**, or **C**) RNA **2**, RNA **3**, and RNA **4**, respectively. Spectra were recorded at a total strand concentration of 0.8 μM and with an excitation wavelength of 340 nm.

(band III/band I $\approx$ 7.0) (entry 1 in Table 3) and Aza-ENA-pyr (**Y**)-modified ODN **4** (band III/band I $\approx$ 1.0) (entry 13 in Table 3), which is to be compared to fluorescence intensity ratio of $\sim$0.6 for band III ($\lambda_{em} \approx$ 396 nm)/band I ($\lambda_{em} \approx$ 376 nm) for the PBA, as a reference, in sodium phosphate buffer (pH 7.0), thereby suggesting that the pyrene-1-yl moiety in the ODNs **1** and **4** is experiencing two different microenvironments. Similar properties were found for other **X**-modified ODNs **2**, **3**, **7**−**10** and **Y**-modified ODNs **5**, **6**, **11**−**14** (entries 7, 10, 25, 28, 31, 34 and 19, 22, 37, 40, 43, 46, respectively, in Table 3) with a small decrease in the intensity ratio of band III/band I for modified ODNs containing dG at the 3′-end of the modification site or dG at both sides of modification. Binding of the **X**-modified ODNs **1**−**3** to the complementary DNA or RNA (entries 2, 3, 8, 9, 11, 12, 26, 27, 29, 30, 32, 33, 35, and 36 in Table 3) resulted in a decrease in the fluorescence intensity ratio of band III/band I $\approx$ 0.9−1.5, with respect to the corresponding single-stranded ODNs. The intensity ratio of band III/band I for the corresponding isosequential ODNs **4**−**6**, **11**−**14** containing **Y** modification in duplexes with complementary DNA or RNA was found to be different from those of corresponding isosequential **X**-modified ODNs, and showed a small increase in the fluorescence intensity ratio of band III/band I $\approx$ 1.0−1.3 (entries 15, 20, 21, 23, 24, 38, 41, 42, 44, 45, 47, and 48 in Table 3) in comparison to the corresponding single-stranded ODNs. Only **Y**-modified ODN **4** containing dT at the 3′-end of the modification site in duplex with complementary DNA showed a small increase in the fluorescence intensity ratio of band III/band I $\approx$ 0.9 (entry 14 in Table 3) with respect to the corresponding single-stranded ODN **4**.

The fluorescence emission spectra for the **X**-modified ODN **1** (inset A) and **Y**-modified ODN **4** (inset B) hybridized with RNAs **2**, **3**, and **4** possessing a single base mismatch (G, U, C, respectively) opposite the modification site in the ODN strand are shown in Figure 4.

The emission spectra of all **X**-modified ODN **1**/RNAs heteroduplexes (entries 4−6 in Table 3) showed unstructured bands with a decrease in fluorescence intensities (measured at $\lambda_{em} \approx$ 376 nm) from $\sim$4.6-fold for (U mismatch) to $\sim$20-fold for (C mismatch) and $\sim$37-fold for (G mismatch) with Φ_F = 0.21−0.79 (entries 4−6 in Table 3) with respect to the duplex with fully match RNA. The fluorescence intensity ratio of band III/band I increased from 0.9 for fully matched ODN **1**/RNA **1** duplex to 2.0−5.7 in the mismatched ODN **1**/RNAs duplexes (entries 4−6 in Table 3).

The **Y**-modified ODN **4**, on the other hand, showed different fluorescent properties upon hybridization with RNA involving G, U, C mismatch opposite to the modification site (entries 16−18 in Table 3). The emission spectra display structure with two vibronic bands, especially in case of G mismatch (inset B in Figure 4), and an increase in fluorescence intensities (measured at $\lambda_{em} \approx$ 385 nm) from $\sim$1.7-fold (U mismatch) to $\sim$2.1-fold (C mismatch) and $\sim$2.7-fold (G mismatch) with Φ_F = 0.21−0.79 (entries 16−18 in Table 3) as compared to the fully match ODN **4**/RNA duplex. The fluorescence intensity ratio of band III/band I decreased from 1.3 for fully matched ODN **4**/RNA **1** duplex to 0.9−1.2 in the mismatched ODN **4**/RNAs duplexes (entries 16−18 in Table 3).

Fluorescence excitation spectra of the Aze-pyr (**X**)-modified ODN **1** and its duplexes with complementary DNA **2**, RNA **1**, and mismatched RNAs **2**−**4** were monitored at 376 nm (inset A in Figure 5). Spectral patterns for the single-stranded ODN **1** and corresponding duplexes with targets were different from each other, indicating different emitting species. Also, only **X**-modified ODN **1**/RNA **1** heteroduplex showed a spectral profile similar to those of free pyrene in aqueous solution.[46] Spectral patterns for the excitation spectra of Aza-ENA-pyr (**Y**)-modified ODN **4** and its duplexes with complementary DNA **2**, RNA **1**, and mismatched RNAs **2**−**4** at 380 nm (inset B in Figure 5), as well as those of the corresponding duplexes with **X**-modified analogue ODN **1**, were substantially different (Figure 5). The large decreases in the intensities are observed for the **X**-modified ODN **1** hybridized with mismatched RNAs **2**−**4** as compared to the matched ODN **1**/DNA **2** and ODN **1**/RNA **1** duplexes. The excitation spectra of **Y**-modified analogues also displayed a change in the fluorescence intensities depending on the nature of target DNA or RNA, showing the strongest peaks for the ODN **4**/DNA **2** homoduplex. These results reflect the changes in the microenvironment around the pyrene moiety brought about by the nature of the conformational

(46) Cho, N.; Asher, S. A. *J. Am. Chem. Soc.* **1993**, *115*, 6349−6356.

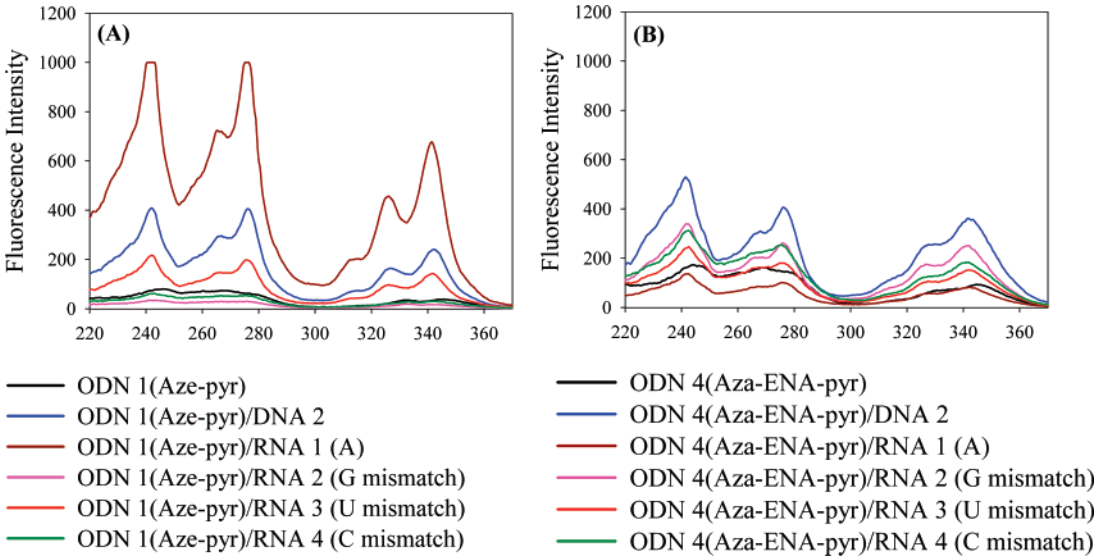

FIGURE 5. Fluorescence excitation spectra of (A) Aze-pyr (**X**)-modified ODN **1** and (B) Aza-ENA-pyr (**Y**)-modified ODN **4** and the corresponding duplexes with complementary DNA **2**, complementary RNA **1**, and single base mismatched (**G**, **U** or **C**) RNA **2**, RNA **3**, and RNA **4**, respectively, obtained by monitoring wavelengths at (A) 376 nm and (B) 380 nm. Spectra were recorded at a total strand concentration of 0.8 μM.

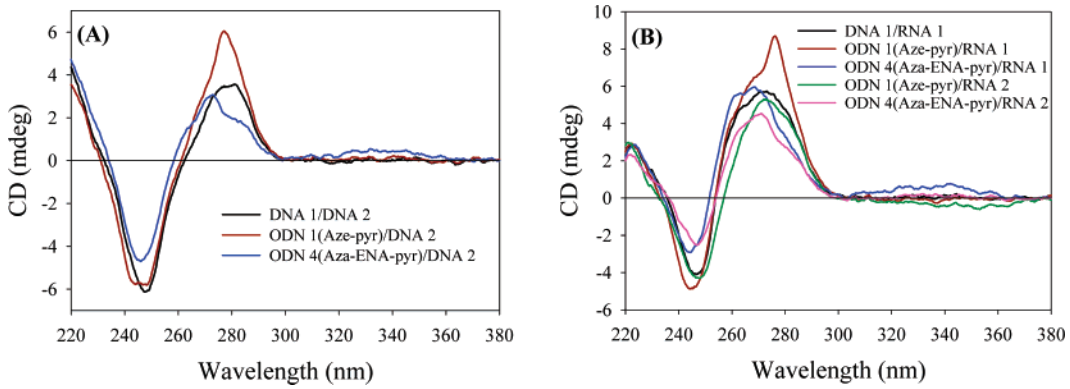

FIGURE 6. (A) CD spectra of duplexes formed by native DNA **1** with complementary DNA **2** and Aze-pyr (**X**)-modified ODN **1** and Aza-ENA-pyr (**Y**)-modified ODN **4** with complementary DNA **2**. (B) CD spectra of duplexes formed by native DNA **1** with complementary RNA **1** and pyrene-modified ODNs **1** and **4** with complementary RNA **1** and with RNA **2** containing single base (**G**) mismatch. The total strand concentration was 10 μM.

constrain imposed at the pyrene chromophore as well as by different nucleobases in the complementary strand opposite to the **X** or **Y**.

2.5. CD Spectra of Pyrene-Modified ODNs and Their Duplexes with DNA and RNA. CD spectra for the **X**-modified ODN **1** and **Y**-modified ODN **4** in duplexes with complementary DNA **2** (inset A in Figure 6) and RNA **1** (inset B in Figure 6) were recorded to examine the detailed structures of the corresponding duplexes. The Aze-pyr-modified ODN **1**/DNA **2** duplex exhibited a CD profile that is similar to that of the unmodified DNA **1**/DNA **2** homoduplex, albeit with an increase of the intensity for the induced CD (ICD) peak at ~278 nm. No ICD absorption was however found at the region between 300 and 380 nm corresponding to the pyrene-chromophore (inset A in Figure 6, Figure S12 in the Supporting Information). In contrast, homoduplex formed by Aza-ENA-pyr-modified ODN **4** and complementary DNA **2** showed relatively weak ICD with a small shift in Cotton peaks to the shorter wavelength. In this case, a positive-induced CD resulting from the pyrene-1-yl unit at the region between 300 and 380 nm was detected (inset A in Figure 6, Figure S12 in the Supporting Information). In both cases, as for the **X**-modified ODN **1**/DNA **2** as well as for the **Y**-modified ODN **4**/DNA **2** duplexes, CD profiles around 260 nm (which reflect the interaction between the transition moments of nucleobases) were slightly modified from that of the native duplex and have a B-like structures.

Upon binding of the **X**-modified ODN **1** to complementary RNA **1**, the CD profile was found to be close to the unmodified heteroduplex DNA **1**/RNA **1** with change of the intensity for the ICD peak at ~278 nm, in the same manner as for the **X**-modified ODN **1**/DNA **2** duplex. Also, no detectable peaks were found in the region corresponding to the pyrene chromophore (inset B in Figure 6, Figure S12 in the Supporting Information). The CD profile for the **Y**-modified ODN **4**/RNA **1** heteroduplex showed ICD similar to the native counterpart, however, with peaks shifted to the shorter wavelength (blue shift) and with positive ICD around 340 nm (inset B in Figure 6, Figure S12 in the Supporting Information). The **X**-modified ODN **1**/RNA **1** duplex and the **Y**-modified ODN **4** in duplex with complementary RNA **1** showed relatively similar global helical conformation with respect to the unmodified hybrid duplex, however differing from each other.

Similar changes in CD profile were detected for other Aze-pyr-modified ODNs **2**−**3** and Aza-ENA-pyr-modified ODNs **5**−**6** upon hybridization with complementary DNA **2** or RNA **1** (Figures S13 and S14 in the Supporting Information). Notably, single-stranded **X**-modified ODN **1** showed negative ICD around 340 nm, whereas no detectable peaks were observed in the same region for the single-stranded **Y**-modified ODN **4** (Figure S15 in the Supporting Information).

Also, we analyzed the CD profiles of two isosequential **X**-modified ODN **1** and **Y**-modified ODNs **4** hybridized with RNA **2** possessing single base (G) mismatch opposite to the modification site, which showed contrasting fluorescence properties (Figure 4). Thus, CD spectra indicate that both heteroduplexes have structures very closely similar to the native double helix of the DNA/RNA heteroduplex (inset B in Figure 6). However, at the region between 300 and 380 nm, the negative ICD was observed for the **X**-modified ODN **1**/RNA **2** duplex and absence of ICD band for the **Y**-modified ODN **4**/RNA **2** duplex (inset B in Figure 6, Figure S12 in the Supporting Information), indicating different stereochemical location and interaction of the pyren-1-yl moiety around the chromophores in the microenvironment in the ODN **1**/RNA **2** or ODN **4**/RNA **2** heteroduplexes.

3. Discussion

3.1. Modulation of Pyrene Fluorescence in the Matched ODN/DNA and ODN/RNA Duplexes by the Nature of Conformational Constraint in the Sugar Moiety. The incorporation of pyrene unit into the specified position of ODNs by covalent attachment to the 2′-*O*-center,[14−16,18,31,32] 2′-*N*-center[47,48] of the sugar, or 2′-*N*-center of the 2′,4′-conformationally constrained residue (such as 2′-amino-LNA)[20,49] has provided fluorescent probes that display strong fluorescence upon hybridization to the target RNA[14−16,18] only, or to both RNA and DNA.[20] In this Article, we have explored the fluorescence properties of ODNs containing conformationally constrained 2′-*N*-(pyren-1-yl)carbonyl-azetidine thymidine, Aze-pyr (**X**), and 2′-*N*-(pyren-1-yl)carbonyl-aza-ENA thymidine, Aza-ENA-pyr (**Y**), modifications (Figure 1) in duplexes with target DNA or RNA.

It has been found that the chemical structure of different conformationally constrained units (Azetidine[35] vs Aza-ENA[36] as in Figure 1) on the sugar moiety brought about a significant difference in fluorescence properties even at the nucleoside level in that the fluorescent quantum yields (Φ_F) of unprotected Aze-pyr-modified nucleoside **3** and Aza-ENA-pyr-modified nucleoside **8** were found to be 0.83 and 0.28, respectively. In both cases, absorption maxima were observed at 341 nm, characteristic of the pyrene chromophore. The incorporation of the corresponding modifications into ODNs (Figure 1) resulted in a fluorescence decrease with $\Phi_F = 0.06-0.73$ for the **X**-modified ODNs **1**−**3**, **7**−**10** and 0.04−0.17 for the **Y**-modified ODNs **4**−**6**, **11**, **13**, and **14** (Table 3), suggesting that the emission of the pyrene in modified ODNs was quenched by the neighboring nucleobases, which are known to be efficient quenchers for pyrene fluorescence via electron transfer from excited pyrene to nucleobases.[42,50] Also, the red shift of absorption maxima for the **X**-modified ODNs **1** (6 nm) and **Y**-modified ODNs **4** (4 nm) (Figure 2) can be consistent with π-stacking involving pyrene and nucleobases, which is known to produce a shift of the absorption to a longer wavelength.[18,46] Only **Y**-modified ODN **12** containing dA at the 3′-end of the modification site displays fluorescence with $\Phi_F = 0.33$ similar to that of Aza-ENA-pyr-modified nucleoside **8**. Upon hybridization with complementary RNA **1**, the **X**-modified ODNs **1**−**3** containing dT at the 3′-end of the modification site displayed structured shape of fluorescence emission with a large increase (up to ∼20-fold) in fluorescence intensity and high quantum yield ($\Phi_F = 0.8-0.85$) (inset A in Figure 3, Table 3). However, only ∼2.5−6-fold increase in fluorescence intensity with $\Phi_F = 0.36-0.40$ appeared for **X**-modified homoduplexes formed with the complementary DNA **2** (Table 3). Blue shift of pyrene absorption band (from 347 to 342 nm for Aze-pyr-modified ODN **1**/RNA **1** and from 347 to 343 nm for ODN **1**/DNA **2** duplexes) (Figure 2) and no ICD in the region between 300 and 380 nm (Figures 6 and S12 in the Supporting Information), in comparison with a negative ICD for the single-stranded **X**-modified ODN (Figure S15 in the Supporting Information), were found for the **X**-modified ODNs **1**−**3** in duplexes with complementary DNA **2** and RNA **1**. It has been shown that a correlation exists between the positive versus negative mode of the ICD signal around 340 nm and the groove binding mode of benzo[*a*]pyrene;[51] thus, a negative ICD is correlated only with an intercalation mode, whereas the positive ICD is correlated with both an external binding and an intercalation mode. This suggests that pyrene-1-yl moiety in our duplexes with complementary DNA **2** or RNA **1** is relatively freer from the π-stacking interaction with the neighboring nucleobases rather than the stacked or intercalation mode found in the single-stranded ODN. The observed decrease in fluorescence intensity ratio of band III/band I from 7.0 for single-stranded ODN **1** to 0.9−1.1 for Aze-pyr-modified ODN **1**/RNA **1** or ODN **1**/DNA **2** duplexes (Table 3) indicates that pyrene-1-yl moiety in these duplexes is located in more hydrophilic environment in comparison to the hydrophobic mode in the single-stranded **X**-modified ODN **1**. Therefore, change of the microenvironment around pyrene-1-yl residue is crucial for the increase in fluorescence intensity in the duplexes. Even though the CD spectra of the DNA and RNA duplexes containing **X** modification did not show a significant difference at the pyrene absorption band, the fluorescence properties and absorption spectra of the corresponding duplexes indicate some difference in pyrene location or interaction mode.

The Aza-ENA-pyr-modified ODN **4** containing dT at the 3′-end of the modification site shows an enhancement of the fluorescence intensity only with the complementary DNA **2** (up to 3.9-fold, $\Phi_F = 0.47$), not with RNA **1** (1.1-fold increase in fluorescence intensity with $\Phi_F = 0.19$) (inset B in Figure 3, Table 3). However, other **Y**-modified ODNs **5**−**6** with the same nucleobase context at the 3′-end of the modification site in duplexes with complementary DNA **2** or RNA **1** displayed similar fluorescence properties (inset B in Figures S2 and S3 in the Supporting Information, Table 3). It is likely that this observation is related to the site-dependency of incorporation of **Y** modification to the ODN, when the modulation of the

(47) Kalra, N.; Babu, B. R.; Parmar, V. S.; Wengel, J. *Org. Biomol. Chem.* **2004**, *2*, 2885−2887.
(48) Kalra, N.; Parlato, M. C.; Parmar, V. S.; Wengel, J. *Bioorg. Med. Chem. Lett.* **2006**, *16*, 3166−3169.
(49) Hrdlicka, P. J.; Babu, B. R.; Sorensen, M. D.; Wengel, J. *Chem. Commun.* **2004**, 1478−1479.
(50) Netzel, T. L.; Zhao, M.; Nafisi, K.; Headrick, J.; Sigman, M. S.; Eaton, B. E. *J. Am. Chem. Soc.* **1995**, *117*, 9119−9128.
(51) Pradhan, P.; Jernstrom, B.; Seidel, A.; Norden, B.; Graslund, A. *Biochemistry* **1998**, *37*, 4664−4673.

microenvironment of the pyrene-1-yl moiety in DNA or RNA duplexes is possible. In contrast to the isosequential **X**-modified ODN **1**, the intensity ratio of band III/band I for the **Y**-modified ODN **4** was found to be similar to the fluorescence intensity ratio of band III/band I for the corresponding **Y**-modified ODN **4**/DNA **2** and ODN **4**/RNA **1** duplexes (Table 3). Also, a small decrease of fluorescence intensity ratio of band III/band I for the Aza-ENA-pyr-modified ODN **4** upon hybridization with complementary DNA **2** suggests that the pyrene was relocated to more hydrophilic area, whereas in heteroduplex with complementary RNA **1** (increase of fluorescence intensity ratio of band III/band I) it was positioned into a more hydrophobic environment. However, the absorption spectra for both **Y**-modified ODN **4**/DNA **2** and ODN **4**/RNA **1** duplexes showed the same small shift of the pyrene absorption maxima (1 nm), with respect to the single-stranded ODN **4**, to the shorter wavelength (Figure 2). In contrast to the **X**-modified duplexes, the CD profile of the duplexes formed by **Y**-modified ODN **4** with complementary DNA **2** or RNA **1** indicates positive ICD in the region between 300 and 380 nm (Figures 6 and S12 in the Supporting Information). This observation can be correlated with the external binding mode or groove-localized pyrene chromophore in ODN **4**/DNA **2** homoduplex (increased fluorescence intensity and decreased intensity ratio of band III/band I). The pyrene-1-yl moiety in ODN **4**/RNA **1** heteroduplex is also localized presumably outside the helix, but has a more hydrophobic environment, as compared to that of ODN **4**/DNA **2** homoduplex, with fluorescence intensity close to the single-strand level and increased fluorescence intensity ratio of band III/band I.

3.2. Modulation of Pyrene Fluorescence in the Matched ODN/DNA and ODN/RNA Duplexes by the Nature of the Neighboring Nucleobase. The other Aze-pyr-modified ODNs **7**−**10** in duplexes with complementary DNA or RNA showed various emission enhancements depending on the nucleobase adjacent to the **X** modification in the ODN (from 5.7-fold increase in fluorescence intensity for ODN **7**/RNA **5** heteroduplex containing dC−rG pair at the 3′-end of the modification site to 26.1-fold increase for the ODN **10**/DNA **6** homoduplex containing dG−dC pair at both sides) with $\Phi_F = 0.13-0.89$ (Table 3). Notably, smaller fluorescence quantum yields ($\Phi_F = 0.13-0.21$) of **X**-modified ODNs **9** and **10** containing dG at the 3′-end of the modification site or at both 3′- and 5′-ends in the duplexes with complementary DNA or RNA, as compared to other ODNs **1**, **7**, and **8**, which have dT, dC, and dA neighbors, respectively, may be correlated with the intercalation mode of pyrene. However, these probes still demonstrate an increase in fluorescence intensity (∼9−26-fold, measured at $\lambda_{em} \approx 376$ nm) upon hybridization with complementary target with respect to the single-stranded ODNs (Table 3). The fluorescent properties of Aza-ENA-pyr-modified ODNs **11**−**14** upon hybridization with complementary DNA or RNA were found to be similar to those of the **Y**-modified ODN **4** containing dT at the 3′-end of the modification site, except ODN **12** (dA at the 3′-end of the modification site), which showed a small drop in fluorescence intensity (Table 3).

3.3. Modulation of Pyrene Fluorescence in the Mismatched ODNs/RNA Duplexes. Recently, studies on fluorescently labeled nucleic acids probes capable of detecting single-base mismatches have been performed in DNA/DNA[17,19,26,37] as well as in RNA/RNA[15] homoduplexes. Among several nucleobases, guanine exhibits exceptionally high quenching efficiency because it is the most electron-donating base, and fluorescence quenching can take place through electron transfer or complex formation with G.[42,52−55] This G-specific quenching has been used in the development of BDF nucleoside (4′PyT), which exhibits intense fluorescence when the 4′PyT is involved in a complementary base pair with A.[19] The Aze-pyr (**X**) and Aza-ENA-pyr (**Y**) modifications (Figure 1) showed extraordinary fluorescence properties in DNA/RNA heteroduplexes possessing single G mismatch in complementary RNA opposite to the modification site. In **X**-modified ODN **1**/RNA **2** heteroduplex, fluorescence intensity was reduced by ∼37-fold ($\Phi_F = 0.21$) with respect to the duplex with fully matched RNA **1**, when Aze-pyr-modified nucleotide in ODN **1** was involved in a base pair with A (inset A in Figure 4, entries 3 and 4 in Table 3). In contrast, the nucleobase mismatch by G instead of A in the RNA strand upon hybridization with **Y**-modified ODN **4** resulted by a ∼3-fold increase in fluorescence intensity with $\Phi_F = 0.27$ (inset B in Figure 4, entries 15 and 16 in Table 3). Other heteroduplexes, involving U or C mismatches, displayed a relatively smaller decrease (for **X**-modified duplexes) or increase (for **Y**-modified duplexes) in fluorescence intensity (Figure 4, Table 3). The fluorescence intensity ratio of band III/band I, which is known to be affected by local environmental polarity,[44,45] was increased (from 0.9 for fully matched to 4.0 for G mismatched) for the **X**-modified ODN **1**/RNA **2** heteroduplex and decreased (from 1.3 for fully matched to 0.9 for G mismatched) for the **Y**-modified ODN **4**/RNA **2** heteroduplex (Table 3). It is suggested that the mode of interaction or location of the pyrene in these heteroduplexes is different. The red shift (from 347 to 351 nm) of the pyrene absorption maximum for the **X**-modified ODN **1** upon hybridization with RNA **2** (G mismatch) (inset A in Figure 2) indicates the stacking interaction between pyrene and nucleobases, when the pyrene-1-yl moiety was in the more hydrophobic environment, whereas a shift to the shorter wavelength of the pyrene absorption maximum (from 345 to 342 nm) appeared for the **Y**-modified ODN **4**/RNA **2** heteroduplex (inset B in Figure 2), indicating relatively poorer stacking interaction as compared to that of the single-stranded ODN **4**, when pyrene chromophore is located in the more hydrophilic environment. These conclusions are in agreement with CD profiles for the corresponding ODN **1**/RNA **2** and ODN **4**/RNA **2** duplexes. The negative ICD at pyrene absorption region was observed for the **X**-modified ODN **1**/RNA **2** (G mismatch) heteroduplex (inset B in Figure 6, Figure S8 in the Supporting Information), suggesting that the pyrene was located in the chiral environment and intercalated; therefore, its absorption was significantly quenched by neighboring G sites. In contrast, no ICD signal at the same region was detected for the **Y**-modified ODN **4**/RNA **2** (G mismatch) heteroduplex (inset B in Figure 6, Figure S8 in the Supporting Information), when, most likely, pyrene was positioned away from the helix, and therefore exhibits enhanced fluorescence.

4. Conclusions

(1) The impact of chemical nature of the conformational constraint in the sugar unit (1′,2′-Azetidine lock vs 2′,4′-Aza-

(52) Knapp, C.; Lecomte, J. P.; Mesmaeker, A. K.; Orellana, G. *J. Photochem. Photobiol., B* **1996**, *36*, 67−76.
(53) Kawai, K.; Takada, T.; Tojo, S.; Ichinose, N.; Majima, T. *J. Am. Chem. Soc.* **2001**, *123*, 12688−12689.
(54) Marras, S. A. E.; Kramer, F. R.; Tyagi, S. *Nucleic Acids Res.* **2002**, *30*, e122/1−e122/8.
(55) Kawai, K.; Yokoohji, A.; Tojo, S.; Majima, T. *Chem. Commun.* **2003**, 2840−2841.

ENA lock) on the modulation of the fluorescence properties of oligodeoxynucleotides containing 2′-*N*-(pyren-1-yl)carbonyl-azetidine thymidine, Aze-pyr (**X**), and 2′-*N*-(pyren-1-yl)carbonyl-aza-ENA thymidine, Aza-ENA-pyr (**Y**), in the duplexes with complementary DNA or matched/mismatched RNA has been described.

(2) The pyrene moiety is presumably outside the helix of the matched nucleic acid duplexes containing dT−d/rA pair at the 3′-end of the modification site for both types of modifications, which can be concluded from the following observations: (i) enhanced fluorescence emission, (ii) small band III/band I intensity ratio, (iii) absence of ICD band or presence of positive ICD band at the pyrene region (340 nm), (iv) blue shift in pyrene absorption maxima with respect to the single-stranded probes, and (v) decrease in the thermal stability of the duplexes.

(3) Pyrene probes display high fluorescence quantum yields for the Aze-pyr-modified ODNs in duplexes with complementary DNA and RNA from 0.13 to 0.89 depending on the nucleobase adjacent to the **X** modification in the ODN. Relatively poorer quantum yields (Φ_F = 0.09−0.47) are however found for the Aza-ENA-pyr-modified ODNs in the DNA and RNA duplexes as compared to conformationally constrained 2′-*N*-(pyren-1-yl)carbonyl conjugated 2′-amino-LNA[20] (Φ_F = 0.34−0.91) for singly pyrene-modified DNA and RNA duplexes.

(4) The specific hybridization-induced increase in fluorescence intensities is from ∼13-fold for ODN/DNA and ∼6-fold for ODN/RNA duplexes for the **X**-modified ODN containing dC at the 3′-end of the modification site and up to ∼26-fold upon hybridization with complementary DNA or ∼23-fold with RNA for the **X**-modified ODN containing dG at both sides of modification. On the other hand, for the **Y**-modified ODNs the fluorescence intensities increase up to 3.9-fold upon hybridization with complementary DNA and only 1.1−1.7-fold with RNA; however, Aza-ENA-pyr probe containing dA at the 3′-end of the modification site showed ∼1.4-fold decrease in fluorescence intensities in ODN/DNA and ODN/RNA duplexes. The above results reflect the relative changes of the microenvironment of pyrene moiety brought about by the chemical nature of the conformationally restricted nucleotide, as well as different structures of the DNA and RNA duplexes.

(5) The intercalation mode of pyrene moiety in the Aze-pyr-modified ODN hybridized with RNA possessing G mismatch is consistent with the following observations: (i) significant decrease in fluorescence intensity (∼37-fold, measured at $\lambda_{em} \approx 376$ nm), (ii) red shift in pyrene absorption maxima with respect to the single-stranded probes, (iii) strong negative ICD at the pyrene region (340 nm), and (iv) large intensity ratio of band III/band I of the emission. In the Aza-ENA-pyr-modified ODN/RNA (with G mismatch in the RNA strand) heteroduplex, the pyrene-chromophore is positioned away from the helix, which is consistent with the following observations: (i) enhanced fluorescence emission, (ii) blue shift in pyrene absorption maxima with respect to the single-stranded probes, (iii) absence of ICD band at the pyrene region, and (iv) decrease in fluorescence intensity ratio of band III/band I.

5. Implication

High quantum efficiency (Φ_F = 0.13−0.89), mismatch discrimination [decrease in fluorescence intensities (measured at $\lambda_{em} \approx 376$ nm) from ∼4.6-fold (U mismatch) to ∼20-fold (C mismatch) and ∼37-fold (G mismatch) with respect to the fully match RNA duplex], and large increase in fluorescence intensity (∼6−23-fold) for the singly Aze-pyr-modified probes upon hybridization with complementary RNA, as compared to the ∼2.5-fold increase for the singly modified probes containing pyrene-functionalized 2′-amino-LNA,[20] can be exploited for monitoring RNA hybridization and RNA folding in general. The fluorescence increase for the pyrene emission of Aza-ENA-pyr (1.4−3.9-fold) as well as Aze-pyr-modified probes (2.7−26.1-fold) in the duplexes with DNA complements and base-mismatch (dT−rA vs dT−rG pair) recognition in the heteroduplexes with RNA [increase in fluorescence intensities for the singly Aza-ENA-pyr-modified ODN from ∼1.7-fold (U mismatch) to ∼2.1-fold (C mismatch) and ∼2.7-fold (G mismatch) with respect to the fully match RNA duplex] can open the way for the design of new base-discriminating fluorescent DNA probes. However, **Y**-modified probes will have limitation if dA is present at the 3′-end of the modification site in the sequence. Also, the destabilizing effect of the **X**-modified probes on the duplex with complementary targets as well as relatively long synthetic pathways for both modifications in general may influence their potential application.

6. Experimental Section

(1*R*,3*R*,4*S*,5*R*)-3-Benzyloxymethyl-4-benzyloxy-6-*N*-(pyren-1-ylcarbonyl)-1-(thymine-1-yl)-6-aza-2-oxabicyclo[3.2.0]heptane (2). To a stirred solution of pyrenecarboxylic acid (0.016 g, 0.064 mmol) in *N*,*N*-dimethylformamide (2 mL) were added (benzotriazol-1-yloxy)tripyrrolidinophosphonium hexafluorophosphate (PyBOP) (0.035 g, 0.067 mmol), diisopropylethylamine (0.01 mL, 0.062 mmol), and nucleoside **1** (0.02 g, 0.044 mmol). The reaction mixture was stirred for 1.5 h at room temperature. Saturated aqueous $NaHCO_3$ solution (5 mL) was added, and the mixture was extracted with dichloromethane (3 × 20 mL). The organic layer was dried over anhydrous $MgSO_4$, filtered, and concentrated in vacuo. The crude product was purified by silica gel column chromatography (0−4% methanol in dichloromethane, v/v) to give **2** (0.026 g, 0.038 mmol, 87%) as a mixture of diastereomers. R_f = 0.39 [96:4 CH_2Cl_2/CH_3OH (v/v)]. MALDI-TOF *m*/*z*: $[M + H]^+$ found, 678.3; calcd, 678.2. ^{13}C NMR (67.9 MHz, $CDCl_3$) δ: 172.6, 163.6, 149.0, 137.6, 135.2, 132.8, 131.0, 130.5, 129.3, 128.9, 128.4, 128.3, 127.7, 127.3, 127.0, 126.3, 126.0, 125.8, 125.4, 124.6, 124.5, 124.2, 123.9, 111.6, 90.0, 82.4, 73.5, 73.2, 69.5, 68.1, 61.3, 12.1.

(1*R*,3*R*,4*S*,5*R*)-3,4-Hydroxy-6-*N*-(pyren-1-ylcarbonyl)-1-(thymine-1-yl)-6-aza-2-oxabicyclo[3.2.0]heptane (3). Compound **2** (0.72 g, 1.06 mmol) dissolved in 20 mL of methanol, $Pd(OH)_2$ on charcoal (20% moist, 0.22 g), and ammonium formate (0.86 g, 13.6 mmol) were added to the solution of nucleoside. The resulting suspension was heated under reflux for 36 h. The reaction mixture was filtered through silica gel bed and washed with hot methanol (40 mL). The filtrate was concentrated to dryness in vacuo and purified by silica gel column chromatography (0−8% methanol in dichloromethane, v/v) to afford **3** (0.41 g, 0.82 mmol, 78%). R_f = 0.34 [90:10 CH_2Cl_2/CH_3OH (v/v)]. MALDI-TOF *m*/*z*: $[M + H]^+$ found, 498.1; calcd, 498.2. ^{13}C NMR (67.9 MHz, CD_3OD) δ: 175.2, 166.7, 151.7, 138.4, 134.5, 132.8, 132.4, 130.6, 130.3, 129.7, 129.4, 128.5, 128.0, 127.6, 127.4, 126.5, 126.1, 125.8, 125.4, 112.3, 91.0, 86.0, 85.0, 74.5, 73.1, 72.0, 70.4, 63.2, 62.6, 62.2, 60.2, 12.4.

(1*R*,3*R*,4*S*,5*R*)-3-(4,4′-Dimethoxytrityloxymethyl)-4-hydroxy-6-*N*-(pyren-1-ylcarbonyl)-1-(thymine-1-yl)-6-aza-2-oxabicyclo-[3.2.0]heptane (4). Nucleoside **3** (0.265 g, 0.53 mmol) was co-evaporated with anhydrous pyridine (3 × 5 mL) and dissolved in 6 mL of the same solvent, and 4,4′-dimethoxytrityl chloride (0.19 g, 0.56 mmol) was added and stirred at room temperature for 12 h under nitrogen atmosphere. The reaction mixture was poured into cold saturated aqueous $NaHCO_3$ solution (10 mL) and extracted with dichloromethane (3 × 30 mL). The organic layer was dried

over anhydrous $MgSO_4$, filtered, and evaporated under reduced pressure followed by co-evaporation with toluene (2 × 20 mL) to remove pyridine partially. The crude product was purified by silica gel column chromatography (0−4% methanol in dichloromethane (v/v), containing 1% pyridine) to give **4** (0.35 g, 0.44 mmol, 82%). R_f = 0.27 [96:4 CH_2Cl_2/CH_3OH (v/v)]. MALDI-TOF *m*/*z*: $[M + H]^+$ found, 800.2; calcd, 800.3. ^{13}C NMR (67.9 MHz, $CDCl_3$ plus DABCO) δ: 173.0, 163.8, 158.4, 149.7, 149.6, 144.7, 135.8, 134.8, 132.8, 131.0, 130.5, 130.0, 129.4, 129.0, 128.1, 127.7, 127.0, 126.7, 126.5, 126.1, 126.0, 124.6, 124.5, 124.4, 124.2, 123.6, 113.0, 111.8, 88.6, 86.2, 84.3, 72.9, 71.9, 62.5, 62.1, 55.1, 46.9, 29.6, 12.3.

(1*R*,3*R*,4*S*,5*R*)-4-(2-Cyanoethoxy(diisopropylamino)-phosphinoxy)-3-(4,4′-dimethoxytrityloxymethyl)-6-*N*-(pyren-1-ylcarbonyl)-1-(thymine-1-yl)-6-aza-2-oxabicyclo[3.2.0]heptane (5). Nucleoside **4** (0.17 g, 0.21 mmol) was dissolved in 3 mL of dry THF, and diisopropylethylamine (0.19 mL, 1.09 mmol) was added at 0 °C under a nitrogen atmosphere followed by 2-cyanoethyl-*N*,*N*-diisopropylphosphoramidochloridite (0.1 mL, 0.45 mmol). After 30 min the reaction was warmed to room temperature and stirred for 1.5 h. Methanol (0.2 mL) was added, and stirring was continued for 10 min, after which the reaction mixture was poured into saturated aqueous $NaHCO_3$ solution (10 mL) and extracted with freshly distilled dichloromethane (3 × 30 mL). The organic layer was dried over anhydrous $MgSO_4$, filtered, and concentrated in vacuo. The crude residue was purified by silica gel column chromatography (20−70% CH_2Cl_2 in cyclohexane containing 2% Et_3N) to afford **5** (0.18 g, 0.18 mmol, 85%) as a mixture of isomers. R_f = 0.39 [96:4 CH_2Cl_2/CH_3OH (v/v)]. MALDI-TOF *m*/*z*: $[M + H]^+$ found, 1000.4; calcd, 1000.4. ^{31}P NMR (67.9 MHz, $CDCl_3$) δ: 149.9, 148.6.

(1*R*,5*R*,7*R*,8*S*)-5-Benzyloxymethyl-8-benzyloxy-2-*N*-(pyren-1-ylcarbonyl)-7-(thymin-1-yl)-2-aza-6-oxabicyclo[3.2.1]octane (7). Chromatography (0−4% methanol in dichloromethane, v/v). Yield: 0.134 g (0.19 mmol, 90%) as a mixture of diastereomers. R_f = 0.35 [96:4 CH_2Cl_2/CH_3OH (v/v)]. MALDI-TOF *m*/*z*: $[M + H]^+$ found, 692.4; calcd, 692.3. ^{13}C NMR (67.9 MHz, $CDCl_3$) δ: 170.8, 170.2, 164.1, 163.5, 162.5, 150.0, 149.9, 137.1, 137.0, 135.4, 134.9, 131.6, 131.5, 130.9, 130.8, 130.5, 130.4, 129.3, 129.2, 128.8, 128.5, 128.4, 128.0, 127.9, 127.7, 127.6, 127.3, 126.9, 126.8, 126.1, 126.0, 125.5, 125.3, 125.1, 124.7, 124.5, 124.2, 124.1, 124.0, 123.7, 123.5, 123.4, 109.9, 107.8, 86.1, 84.6, 84.2, 73.4, 73.2, 72.9, 72.4, 72.2, 71.6, 71.3, 69.6, 69.3, 67.3, 62.4, 56.1, 56.0, 48.1, 48.0, 41.6, 41.1, 36.3, 35.9, 31.3, 29.5, 27.3, 26.8, 26.3, 25.8, 25.7, 11.9, 11.5.

(1*R*,5*R*,7*R*,8*S*)-5,8-Hydroxy-2-*N*-(pyren-1-ylcarbonyl)-7-(thymin-1-yl)-2-aza-6-oxabicyclo[3.2.1]octane (8). Chromatography (0−8% methanol in dichloromethane, v/v). Yield: 0.081 g (0.16 mmol, 82%). R_f = 0.35 [90:10 CH_2Cl_2/CH_3OH (v/v)]. MALDI-TOF *m*/*z*: $[M + H]^+$ found, 512.4; calcd, 512.2. ^{13}C NMR (67.9 MHz, DMSO-d_6) δ: 169.7, 168.8, 164.3, 163.6, 150.3, 149.6, 135.7, 135.2, 131.0, 130.9, 130.7, 130.6, 130.4, 130.2, 128.3, 128.0, 127.8, 127.6, 127.3, 127.2, 126.8, 126.6, 126.4, 126.3, 125.8, 125.7, 125.6, 125.4, 125.1, 125.0, 124.9, 124.7, 124.6, 124.0, 123.9, 123.8, 123.7, 108.0, 107.8, 107.6, 85.6, 85.3, 85.2, 64.3, 64.0, 63.4, 63.2, 63.0, 60.9, 58.5, 54.9, 42.0, 41.5, 36.1, 35.6, 34.7, 27.3, 26.0, 25.3, 25.0, 12.5, 12.3.

(1*R*,5*R*,7*R*,8*S*)-5-(4,4′-Dimethoxytrityloxymethyl)-8-hydroxy-2-*N*-(pyren-1-ylcarbonyl)-7-(thymin-1-yl)-2-aza-6-oxabicyclo-[3.2.1]octane (9). Chromatography (0−4% methanol in dichloromethane (v/v), containing 1% pyridine). Yield: 0.06 g (0.074 mmol, 76%). R_f = 0.22 [96:4 CH_2Cl_2/CH_3OH (v/v)]. MALDI-TOF *m*/*z*: $[M + H]^+$ found, 814.2; calcd, 814.3. ^{13}C NMR (67.9 MHz, $CDCl_3$ plus DABCO) δ: 171.3, 171.2, 164.7, 163.3, 158.5, 150.2, 149.7, 144.3, 144.0, 135.5, 135.2, 134.8, 131.7, 131.1, 130.8, 130.6, 130.0, 129.1, 128.9, 128.1, 127.9, 127.7, 127.0, 126.8, 126.3, 126.2, 125.7, 125.5, 124.6, 124.3, 123.5, 113.2, 110.3, 110.0, 86.7, 86.4, 85.9, 85.7, 85.4, 85.1, 68.0, 66.6, 65.2, 64.1, 63.5, 63.3, 59.4, 59.3, 55.1, 51.2, 46.1, 43.2, 42.2, 41.8, 40.6, 36.0, 34.9, 29.6, 27.1, 26.7, 26.3, 25.5, 12.1, 11.7.

(1*R*,5*R*,7*R*,8*S*)-8-(2-Cyanoethoxy(diisopropylamino)-phosphinoxy)-5-(4,4′-dimethoxytrityloxymethyl)-2-*N*-(pyren-1-ylcarbonyl)-7-(thymin-1-yl)-2-aza-6-oxabicyclo[3.2.1]octane (10). Chromatography (20−70% CH_2Cl_2 in cyclohexane containing 2% Et_3N). Yield: 0.11 g (0.11 mmol, 73%) as a mixture of isomers. R_f = 0.34 [96:4 CH_2Cl_2/CH_3OH (v/v)]. MALDI-TOF *m*/*z*: $[M + H]^+$ found, 1014.4; calcd, 1014.4. ^{31}P NMR (67.9 MHz, $CDCl_3$) δ: 153.3, 151.6, 150.1, 149.5.

Oligonucleotide Synthesis. All ODNs were synthesized by the conventional phosphoramidite method[38] by using a DNA/RNA synthesizer. Standard procedures were used to synthesize ODNs except for extended coupling time (10 min, DCI as an activator) for phosphoramidite containing 2′-*N*-(pyren-1-yl)carbonyl-azetidine unit and 2′-*N*-(pyren-1-yl)carbonyl-aza-ENA unit (coupling time 10 min, ETT as an activator). RNA synthesis was performed by standard procedures[56,57] using 2′-*O*-tBDMS as 2′-OH protecting group and ETT as an activator with coupling time of 120 s. The ODNs were cleaved from solid support and deprotected from nucleobase protecting group using 32% aqueous ammonia at room temperature for 24 h. Deprotection of the oligo-RNAs was carried out using anhydrous methanolic ammonia (25% NH_3/MeOH) at 55 °C for 16 h followed by 1 M TBAF/THF treatment. All ONs were purified by PAGE (20% polyacrylamide/7 M urea), extracted with 0.3 M NaOAc, and desalted with C18-reverse phase cartridges. Purity of products was confirmed by PAGE and was greater than 95%. Each ON was verified by MALDI-TOF MS (Table S1 in the Supporting Information). Concentration of ODNs containing 2′-*N*-(pyren-1-yl)carbonyl-azetidine unit or 2′-*N*-(pyren-1-yl)carbonyl-aza-ENA unit was determined accounting for the contribution to the absorbance at 260 nm from the (pyren-1-yl)carbonyl- moiety. The molar extinction coefficient (ϵ*) for modified ODNs **1**−**14** was calculated from the extinction coefficient (ϵ) for the corresponding ODNs using the equation:

$$\epsilon^* = \epsilon \times \frac{A_{260}/A_{340}}{A_{260}/A_{340} - A_{260}^*/A_{340}^*}$$

where A_{260} and A_{340} are the absorbance of Aze-pyr (**X**)- or Aza-ENA-pyr (**Y**)-modified ODNs at 260 and 340 nm, respectively; A_{260}* and A_{340}* are the absorbance of pyrenecarboxylic acid at 260 and 340 nm, respectively.

UV Melting Experiments. Determination of the T_m's of the ODNs/RNA or ODNs/DNA hybrid duplexes was carried out in medium salt buffer, containing 100 mM NaCl (pH 7.0, adjusted with 10 mM NaH_2PO_4/5 mM Na_2HPO_4) and 0.1 mM EDTA. Absorbance was monitored at 260 nm in the temperature range from 15 to 70 °C with ramp of 1 °C per min. Samples (mixture of 1.0 μM ODN and 1.0 μM RNA or DNA) were denatured at 80 °C for 4 min followed by slow cooling to 15 °C prior to the measurements. T_m values were obtained from the maxima of the first derivatives of the melting curves. All thermal denaturation temperatures given are the averages of at least of two independent sets of experiments and are within ±0.2 °C error range.

UV Absorption and Fluorescence Measurements, and CD Experiments. Oligonucleotides solutions were prepared as described in UV melting experiments (19.5 μM for ODNs **1**−**6** and 9.75 μM for ODNs **7**−**14**, final strand concentration). Absorption spectra were obtained at 25 °C using 1.0 cm path length cell. For the fluorescence measurements above, samples were diluted with the same buffer to the concentration of 0.8 μM of strands, and spectra were obtained at 20 °C (±0.1 °C) using quartz optical cell with a path length of 1.0 cm. Fluorescence emission spectra (excitation wavelength of 340 nm) and excitation spectra (monitoring wavelength at 376 and 380 nm) were obtained as an average

(56) Sproat, B.; Colonna, F.; Mullah, B.; Tsou, D.; Andrus, A.; Hampel, A.; Vinayak, R. *Nucleosides Nucleotides* **1995**, *14*, 255−273.
(57) Milecki, J.; Zamaratski, E.; Maltseva, T. V.; Foldesi, A.; Adamiak, R. W.; Chattopadhyaya, J. *Tetrahedron* **1999**, *55*, 6603−6622.

of five scans using an excitation slit of 4.0 nm, emission slit of 2.5 nm, and scan speed of 500 nm/min. Corrections were made for solvent background, but no attempts were made to eliminate dissolved oxygen in the buffer solution for the fluorescence measurements. The fluorescence quantum yields [Φ_F(ODN)] of pyrene-labeled ODNs were determined according to:[41]

$$\Phi_F(\text{ODN}) = [A_{340}(\text{PBA})/A_{340}(\text{ODN})] \times [F(\text{ODN})/F(\text{PBA})] \times [n(H_2O)/n(\text{MeOH})]^2 \times \Phi_F(\text{PBA})$$

where Φ_F(PBA) is the fluorescence quantum yield of PBA as a reference with a known Φ_F of 0.065;[42,43] A_{340} is the absorbance of the sample at the excitation wavelength (340 nm); F is the area of the fluorescence emission spectra of the sample from 360 to 590 nm; and $n(H_2O)$ and n(MeOH) are the refractive indexes of water (1.3328) and methanol (1.3288). Fluorescence quantum yields were determined as an average of minimum two measurements within ±10% error range. For CD experiments, oligonucleotide solutions were prepared as described in UV melting experiments (10 μM, final strand concentration). CD spectra were recorded from 380 to 220 nm at 25 °C using 0.2 cm path length cell. Spectra were obtained as an average of five scans from which the CD spectrum of buffer was subtracted.

Acknowledgment. Generous financial support from the Swedish Natural Science Research Council (Vetenskapsrådet), the Swedish Foundation for Strategic Research (Stiftelsen för Strategisk Forskning), and the EU-FP6 funded RIGHT project (project no. LSHB-CT-2004-005276) is gratefully acknowledged. We would like to thank Dr. J. Barman for MALDI-TOF MS analysis.

Supporting Information Available: General experimental methods; experimental conditions for the preparation of 2′-*N*-(pyren-1-yl)carbonyl-aza-ENA thymidine and its phosphoramidite building block; MALDI-TOF MS of synthesized ONs; absorption spectra of fully deprotected nucleosides **3** and **8**; fluorescence emission spectra of **X**-modified ODN **2**−**3** and **Y**-modified ODN **5**−**6**; area versus A_{340} curves for the determination of the emission quantum yields of fully deprotected nucleosides **3** and **8**; fluorescence emission spectra for the temperature-dependent fluorescence changes of the duplexes formed by ODN **1** or ODN **4** with complementary target; fluorescence emission spectra of ODNs **7**−**14**; expanded CD spectra of the duplexes formed by ODNs **1** or **4** with complementary DNA, RNA, and mismatched (**G**) RNA; CD spectra of the native, **X**-modified, and **Y**-modified DNA/DNA and DNA/RNA duplexes; ^{1}H NMR spectra of compounds **2**−**4** and **7**; ^{13}C NMR spectra of compounds **1**−**4**, **6**−**9**; and ^{31}P NMR spectra of compounds **5** and **10**. This material is available free of charge via the Internet at http://pubs.acs.org.

JO702747W